Degrees of Freedom and Achievable Rate of Wide-Band Multi-Cell Multiple Access Channels With No CSIT

Yo-Seb Jeon, Namyoon Lee, *Member, IEEE*, and Ravi Tandon, *Senior Member, IEEE*

***Abstract*— This paper considers a *K*-cell multiple access channel with inter-symbol interference. The primary finding of this paper is that, without instantaneous channel state information at the transmitters, *interference-free degrees-of-freedom (DoF) per cell* is achievable, provided that the delay spread of the desired links is significantly longer than that of the interfering links when the number of user per cell is sufficiently large. This achievability is shown by a blind interference management method that exploits the relativity in delay spreads between desired and interfering links. In this method, all inter-cell-interference signals are aligned-and-cancelled by using discrete-Fourier-transform-based precoding and combining, both depend only on the lengths of channel-impulse-response. In addition to the DoF analysis, the achievable rate of the proposed method is characterized in a closed-form expression. Some illustrative examples are presented to show an additional sum-DoF gain obtained by exploiting propagation delay in the interfering links or the heterogeneity of the channel coherence time between the desired and interfering links.**

***Index Terms*— Multiple access channel (MAC), interfering MAC, inter-symbol interference (ISI), blind interference management.**

I. Introduction

MULTI-CELL multiple access channel (MAC) with inter-symbol interference captures the communication scenario in which multiple uplink users per cell communicate with their associated base stations (BSs) by utilizing the same time and frequency resources across both the users and the BSs. The spectral efficiency of this channel is fundamentally limited by three different types of interference:

- Inter-cell interference (ICI), which arises from simultaneous transmissions of users in neighboring cells;
- Inter-user-interference (IUI), which is caused by simultaneous transmissions of multiple users in the same cell; and
- Inter-symbol-interference (ISI), which occurs by the relativity between the transmit signal's bandwidth and the coherence bandwidth of a wireless channel.

Orthogonal frequency division multiple access (OFDMA) is the most well-known approach to mitigate both IUI and ISI in the multi-cell systems [2]–[4]. The key idea of OFDMA is to decompose a wideband (frequency-selective) channel into multiple orthogonal narrowband (frequency-flat) subchannels, each with no ISI. By allocating non-overlapping sets of subchannels to the users in a cell, each user is able to send information data without suffering from ISI and IUI in the cell. For instance, in a two-user MAC with ISI, which captures a single-cell uplink communication scenario, the capacity has been characterized by finding an optimal power allocation strategy across the subchannels [5]–[7]. These approaches, however, still suffer from ICI, which is a major hindrance towards increasing the spectral efficiency in multi-cell scenarios.

Multi-cell cooperation has been considered as an effective solution to manage ICI problems for future cellular networks where BSs are densely deployed and small cells overlap heavily with macrocells [8]–[10]. The common idea of multi-cell cooperation is to form a BS cluster, which allows the information exchange among the BSs within the cluster, in order to jointly eliminate ICI. When multiple BSs in a cluster perfectly share the received uplink signals and channel state information (CSI) with each other via capacity-unlimited backhaul links, it is theoretically possible to eliminate ICI completely within the cluster. One problem with implementing multi-cell cooperation is that cooperation of an entire network is not feasible considering the prohibited cost to establish high-capacity backhaul links. As a practical solution, one could define multiple sets of BSs, multiple BS clusters, over an entire network, in which the BSs in a cluster are connected by high-capacity backhaul links. In this case, users (or BSs) outside the cluster are sources of interference, and this poses a fundamental limit to multi-cell cooperation even with capacity-unlimited backhaul links per cluster. Another problem of multi-cell cooperation is that the amount of information that can be exchanged among BSs could be restricted due to capacity-limited backhual links. This possibly leads to the severe spectral efficiency loss that is caused by residual ICI.

Manuscript received April 6, 2017; revised September 3, 2017 and November 27, 2017; accepted December 6, 2017. Date of publication December 14, 2017; date of current version April 16, 2018. The work of N. Lee was supported by the Institute for Information & communications Technology Promotion (IITP) under grant funded by the MSIT of the Korea government [2017(2016-0-00123)]. The work of R. Tandon was supported by US NSF through grants CCF-1559758 and CNS-1715947. The associate editor coordinating the review of this paper and approving it for publication was S. Bhashyam. *(Corresponding author: Namyoon Lee.)*

Y.-S. Jeon and N. Lee are with the Department of Electrical Engineering, Pohang University of Science and Technology, Pohang 37673, South Korea (e-mail: yoseb.jeon@postech.ac.kr; nylee@postech.ac.kr).

R. Tandon is with the Department of Electrical and Computer Engineering, University of Arizona, Tucson, AZ 85721 USA (e-mail: tandonr@email.arizona.edu).

Color versions of one or more of the figures in this paper are available online at http://ieeexplore.ieee.org.

Digital Object Identifier 10.1109/TCOMM.2017.2783625

Among multi-cell cooperation strategies, coordinated beamforming provides a good tradeoff between the overheads for the information exchange and the gains on the spectral efficiency because this strategy only requires CSI exchange among the BSs in the same cluster [11], [12]. Interference alignment (IA) is a representative coordinated beamforming method, which aligns ICI in a subspace so that the signal dimension occupied by interference is confined [13], [14]. For example, in a single-input-single-output (SISO) interference channel, IA has shown to be an optimal strategy in the sense of sum degrees-of-freedom (DoF) that characterizes the approximate sum-spectral efficiency in a high signal-to-noise-ratio (SNR) regime [14]. The concept of IA has also been extended to multi-cell MACs (or interfering MACs) in single antenna settings [15], [16] and multiple antenna settings [18]–[20]. One remarkable result is that, by an uplink IA method, the sum-DoF of K is asymptotically achievable in the K-cell SISO MAC as the number of uplink users per cell approaches infinity [15]–[17]. The common requirement of prior works in [14]–[20] is global and perfect CSI at a transmitter (CSIT), which is a major obstacle in implementing these IA methods in practice.

Recently, IA techniques using limited CSIT have extensively developed for various scenarios such as delayed CSIT [22], mixed CSIT [23], alternating CSIT [24]–[26], one-bit CSIT [27], and no CSIT [28], [29] (see the references therein [22]–[30]). Representatively, blind IA introduced by [31]–[33] has been considered as a practical IA technique when using limited CSIT. An attractive feature of blind IA is that it only requires to know autocorrelation functions of the channels in both time and frequency domains. This technique, however, heavily relies on the existence of the certain structure of channel coherence patterns, which may not be applicable for practical wireless environments in general.

All the aforementioned multi-cell cooperation strategies have focused on the mitigation of ICI under the premise of perfect IUI and ISI cancellation by OFDMA. Recently, a blind interference management method has been proposed for the K-user SISO interference channel with ISI [34]. The key idea of this method is to exploit the relativity of multi-path-channel lengths between desired and interfering links. This channel relativity allows the ICI alignment with discrete Fourier transform (DFT)-based precoding that needs no CSIT. One remarkable result in [34] is that, without instantaneous CSIT, the sum-DoF of the K-user interference channel can be made to scale linearly with the number of communication pairs K, under some conditions on ISI channels.

In this paper, we consider the K-cell SISO MAC with ISI, as illustrated in Fig. 1. Continuing in the same spirit with [34], we attempt to characterize the sum-DoF of the multi-cell MAC with ISI in the absence of CSIT. Our major contribution is to demonstrate that, without instantaneous CSIT, the sum-DoF of the considered channel is

$$\left(1-\frac{L_{\rm I}}{L_{\rm D}}\right)K,$$

provided that $L_{\rm D} \geq 2(L_{\rm I}-1)$ and the number of users per cell is larger than $L_{\rm D}-L_{\rm I}$, where $L_{\rm D}$ and $L_{\rm I}$ are the

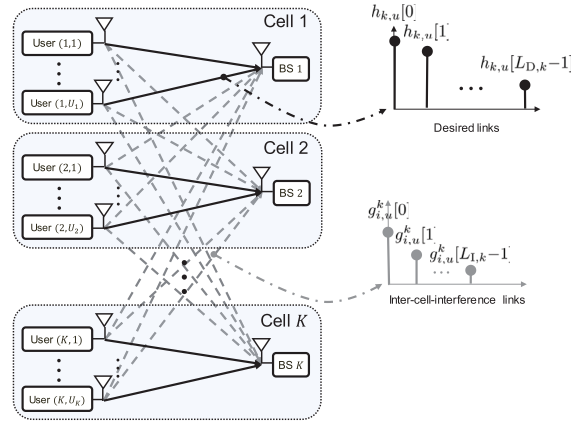

Fig. 1. An illustration of the system model for a K-cell MAC with ISI, in which U_k users are associated with the k-th BS.

channel-impulse-response (CIR) lengths of desired and ICI links in each cell, respectively. Our result implies that *interference-free DoF per cell* (i.e., sum-DoF of K) is achievable as $\frac{L_{\rm D}}{L_{\rm I}}$ approaches infinity with a sufficiently large number of users per cell. This result extends the sum-DoF result in [34], where the sum-DoF of $\frac{K}{2}$ is shown to be achievable without CSIT when each BS communicates with a single user. Therefore, our result also shows that communicating with multiple users in a cell provides a significant DoF gain compared to the single-user case, even in the absence of CSIT.

To demonstrate our result, we develop a blind interference management method by modifying the method in [34] for the multi-cell MAC with ISI. Then we present a new decodability proof to characterize the sum-DoF gain obtained from multiple users. The underlying idea of the developed method is to exploit the heterogeneity of multi-path channel delay spreads between desired and ICI links. We exploit this heterogeneity to create non-circulant channel matrices for the desired links, while generating circulant channel matrices for the ICI links. This strategy, jointly with the property of circulant matrices, allows us to cancel all ICI signals by using DFT-based precoding and combining, even in the absence of instantaneous CSIT. After the ICI cancellation, each BS reliably decodes data symbols sent from the associated users under the premise that local CSI at a receiver (CSIR) is available. We prove the decodability of the data symbols at the BS, by using the property of the DFT matrix. Our decodability proof reveals that the sum-DoF gain compared to the original method in [34] is obtained from channel diversity provided by the joint transmission of multiple users. In addition to the sum-DoF, we also characterize the achievable rate of the proposed method in a closed-form. Using some illustrative examples, we demonstrate that the sum-DoF of this method can be further improved by exploiting propagation delays in the ICI link or the heterogeneity of the channel coherence time between the desired and ICI links.

The blind interference management method developed in this paper was first presented in [1] by the authors of this work. A major limitation of the method in [1] is that it supports only the transmission of a single data stream per user, so the achievable sum-DoF is shown under a constraint on the number of users per cell. Our contributions compared to [1] are 1) to generalize the method in [1] to support the transmission of multiple data streams per user, and 2) to derive the sum-DoF of the generalized method that relaxes the constraint assumed in [1].

Notation: Upper-case and lower-case boldface letters denote matrices and column vectors, respectively. $\mathbb{E}[\cdot]$ is the statistical expectation, $\Pr(\cdot)$ is the probability, $(\cdot)^\top$ is the transpose, $(\cdot)^H$ is the conjugate transpose, $\lceil\cdot\rceil$ is the ceiling function, $\lfloor\cdot\rfloor$ is the floor function, and $(x)^+ = \max\{x, 0\}$. $\mathbf{I}_m$ is an $m \times m$ identity matrix, $\mathbf{1}_{m\times n}$ is an $m \times n$ all-one matrix, and $\mathbf{0}_{m\times n}$ is an m by n all-zero matrix. $|\cdot|$ has three different meanings: $|a|$ denotes the absolute value of a scalar a; $|\mathcal{A}|$ denotes the cardinality of a set $\mathcal{A}$; and $|\mathbf{A}|$ denotes the determinant of a matrix $\mathbf{A}$.

II. System Model

We consider a K-cell SISO MAC with ISI, where U_k uplink users attempt to access a BS in cell k for $k \in \mathcal{K} \triangleq \{1, 2, \ldots, K\}$, by using the common time-frequency resources. We denote $\mathcal{U}_k$ as the index set of users associated with the k-th BS and (k, u) be the index of the u-th user in cell k. We assume that all users and BSs are equipped with a single antenna. We assume that the channel impulse response (CIR) between a user (a transmitter) and a BS (a receiver) is modeled with a finite number of taps. We denote $L_{\mathrm{D},k}$ and $L_{\mathrm{I},k}$ as the number of the CIR taps of the desired and ICI links associating with the k-th BS, respectively. We model the CIR of the desired link between user (k, u) and the k-th BS by $\{h_{k,u}[\ell]\}_{\ell=0}^{L_{\mathrm{D},k}-1}$, while modeling the CIR of the ICI link between user (i, u) and the k-th BS for $i \neq k$ by $\{g_{i,u}^k[\ell]\}_{\ell=0}^{L_{\mathrm{I},k}-1}$. Note that the number of the CIR taps is typically determined as $\left\lceil T_{i,u}^{\mathrm{D},k} W_{\mathrm{BW}} \right\rceil$, where W_{BW} is the transmission bandwidth of the system, and $T_{i,u}^{\mathrm{D},k}$ is the delay spread of the wireless channel from user (i, u) to the k-th BS.

We assume a block-fading channel model in which CIR taps are time-invariant during each block transmission. We also assume that each CIR tap is independently drawn from a continuous distribution. For example, in a rich-scattering propagation environment, CIR taps can be modeled as circularly symmetric complex Gaussian random variables.

Let $x_{k,u}[n]$ be the transmitted signal of user (k, u) at time slot n with the power constraint of $\mathbb{E}[|x_{k,u}[n]|^2] = P$. Then the received signal of the k-th BS at time slot n is

$$y_k[n] = \sum_{u=1}^{U_k} \sum_{\ell=0}^{L_{\mathrm{D},k}-1} h_{k,u}[\ell] x_{k,u}[n-\ell] + \sum_{i\neq k} \sum_{u=1}^{U_i} \sum_{\ell=0}^{L_{\mathrm{I},k}-1} g_{i,u}^k[\ell] x_{i,u}[n-\ell] + z_k[n], \quad (1)$$

where $z_k[n]$ is noise at the k-th BS in time slot n. We assume that $z_k[n]$ is independent and identically distributed (IID) circularly symmetric complex Gaussian random variable with zero mean and variance σ^2, i.e., $\mathcal{CN}(0, \sigma^2)$.

Throughout the paper, we assume no instantaneous CSIT, implying that all users (transmitters) do not have any knowledge of CIR taps. Furthermore, we assume that each BS is available to access knowledge of CIR taps of the desired link, i.e., $\{h_{k,u}[\ell]\}_{\ell=0}^{L_{\mathrm{D},k}-1}$ for $k \in \mathcal{K}$. This is referred to as local CSIR. Note that local CSIR is necessary to perform coherent detection at the BSs.

Definition (Sum Degrees of Freedom): Similar to [13] and [14], we define a sum degrees-of-freedom (sum-DoF), which characterizes the behavior of the sum-spectral efficiency of the system at high SNR. User (k, u) sends an independent message $m_{k,u}(P)$ to the associated BS during T time slots. In this case, the rate of user (k, u) is given by $R_{k,u}(P) = \frac{\log_2 |m_{k,u}(P)|}{T}$. The rate $\sum_{u=1}^{U_k} R_{k,u}(P)$ is *achievable* if the k-th BS is able to decode the transmitted messages from the associating users with an arbitrarily-small error probability by choosing a sufficiently large T. Then the DoF of the k-th BS is defined as

$$d_k = \lim_{P\to\infty} \frac{\sum_{u=1}^{U_k} R_{k,u}(P)}{\log_2(P)} = \lim_{P\to\infty} \frac{\sum_{u=1}^{U_k} \log_2 |m_{k,u}(P)|}{T \log_2(P)}, \quad (2)$$

and the *sum-DoF* is defined as $d_\Sigma = \sum_{k=1}^{K} d_k$.

III. Blind Interference Management Using Channel Structural Relativity

In this section, using a simple example scenario, we present the key concept of the proposed interference management method that exploits channel structural relativity. The generalization of this method will be presented in the sequel, to derive our main result.

Example 1 (K-Cell MAC With Two Users): We consider a K-cell MAC with two users per cell. We assume that delay spreads of wireless channels for different cells are symmetric where the number of CIR taps of the desired link is four, while that of the ICI link is two, i.e., $L_{\mathrm{D},k} = L_{\mathrm{D}} = 4$ and $L_{\mathrm{I},k} = L_{\mathrm{I}} = 2$ for $k \in \mathcal{K} \triangleq \{1, 2, \ldots, K\}$. In this scenario, we show that it is possible to reliably decode total $2K$ data symbols with four time slots, i.e., $d_\Sigma = \frac{2K}{4} = \frac{K}{2}$, without CSIT. The principal idea of the proposed interference management method is to exploit relativity in delay spreads between desired and ICI links to align all ICI signals to the same direction without instantaneous CSIT.

Let all users use a common precoding vector $\mathbf{f}_1 = \frac{1}{\sqrt{3}}[1, 1, 1]^\top$ to send a data symbol. Then the precoded signal vector of user (k, u), $\bar{\mathbf{x}}_{k,u} \in \mathbb{C}^3$, is

$$\bar{\mathbf{x}}_{k,u} = \left[x_{k,u}[1], x_{k,u}[2], x_{k,u}[3]\right]^\top = \mathbf{f}_1 s_{k,u}. \quad (3)$$

By appending one zero at the end of $\bar{\mathbf{x}}_{k,u}$ in (3), the transmitted signal vector of user (k, u) is

$$\mathbf{x}_{k,u} = \left[\bar{\mathbf{x}}_{k,u}, 0\right]^\top = \left[x_{k,u}[1], x_{k,u}[2], x_{k,u}[3], 0\right]^\top. \quad (4)$$

According to the above transmission strategy, every user uses four time slots to send one data symbol. The received signal vector of the k-th BS during four time slots are given by

$$\underbrace{\begin{bmatrix} y_k[1] \\ y_k[2] \\ y_k[3] \\ y_k[4] \end{bmatrix}}_{\mathbf{y}_k} = \sum_{u=1}^{2} \underbrace{\begin{bmatrix} h_{k,u}[0] & 0 & 0 \\ h_{k,u}[1] & h_{k,u}[0] & 0 \\ h_{k,u}[2] & h_{k,u}[1] & h_{k,u}[0] \\ h_{k,u}[3] & h_{k,u}[2] & h_{k,u}[1] \end{bmatrix}}_{\mathbf{H}_{k,u}^{k}} \bar{\mathbf{x}}_{k,u}$$
$$+ \sum_{i\neq k}^{K} \sum_{u=1}^{2} \underbrace{\begin{bmatrix} h_{i,u}^{k}[0] & 0 & 0 \\ h_{i,u}^{k}[1] & h_{i,u}^{k}[0] & 0 \\ 0 & h_{i,u}^{k}[1] & h_{i,u}^{k}[0] \\ 0 & 0 & h_{i,u}^{k}[1] \end{bmatrix}}_{\mathbf{H}_{i,u}^{k}} \bar{\mathbf{x}}_{i,u} + \underbrace{\begin{bmatrix} z_k[1] \\ z_k[2] \\ z_k[3] \\ z_k[4] \end{bmatrix}}_{\mathbf{z}_k}. \quad (5)$$

Let $\mathbf{D}_k$ be a linear combining matrix used at the receiver, defined as

$$\mathbf{D}_k = \begin{bmatrix} 1 & 0 & 0 & 1 \\ 0 & 1 & 0 & 0 \\ 0 & 0 & 1 & 0 \end{bmatrix}. \quad (6)$$

Then using $\mathbf{D}_k$, the combined received vector of the k-th BS, namely $\bar{\mathbf{y}}_k$, is obtained as

$$\bar{\mathbf{y}}_k = \mathbf{D}_k \mathbf{y}_k = \sum_{u=1}^{2} \underbrace{\begin{bmatrix} h_{k,u}[0]+h_{k,u}[3] & h_{k,u}[2] & h_{k,u}[1] \\ h_{k,u}[1] & h_{k,u}[0] & 0 \\ h_{k,u}[2] & h_{k,u}[1] & h_{k,u}[0] \end{bmatrix}}_{\bar{\mathbf{H}}_{k,u}} \bar{\mathbf{x}}_{k,u}$$
$$+ \sum_{i\neq k} \sum_{u=1}^{2} \underbrace{\begin{bmatrix} g_{i,u}^{k}[0] & 0 & g_{i,u}^{k}[1] \\ g_{i,u}^{k}[1] & g_{i,u}^{k}[0] & 0 \\ 0 & g_{i,u}^{k}[1] & g_{i,u}^{k}[0] \end{bmatrix}}_{\bar{\mathbf{G}}_{i,u}^{k}} \bar{\mathbf{x}}_{i,u}$$
$$+ \underbrace{\begin{bmatrix} z_k[1] + z_k[4] \\ z_k[2] \\ z_k[3] \end{bmatrix}}_{\bar{\mathbf{z}}_k}. \quad (7)$$

An important observation in (7) is that all interference channel matrices $\bar{\mathbf{G}}_{i,u}^{k}$ for $i \neq k$ become circulant. Meanwhile, desired channel matrices $\bar{\mathbf{H}}_{k,u}$ can be expressed as a superposition of circulant and noncirculant matrices as follows:

$$\bar{\mathbf{H}}_{k,u} = \underbrace{\begin{bmatrix} h_{k,u}[0] & h_{k,u}[2] & h_{k,u}[1] \\ h_{k,u}[1] & h_{k,u}[0] & h_{k,u}[2] \\ h_{k,u}[2] & h_{k,u}[1] & h_{k,u}[0] \end{bmatrix}}_{\bar{\mathbf{H}}_{k,u}^{\mathrm{C}}} + \underbrace{\begin{bmatrix} h_{k,u}[3] & 0 & 0 \\ 0 & 0 & -h_{k,u}[2] \\ 0 & 0 & 0 \end{bmatrix}}_{\bar{\mathbf{H}}_{k,u}^{\mathrm{NC}}}. \quad (8)$$

Since a circulant matrix is diagonalized by DFT matrix, $\bar{\mathbf{G}}_{i,u}^{k}$ in (7) is rewritten as

$$\bar{\mathbf{G}}_{i,u}^{k} = \left[\mathbf{f}_1 \ \ \mathbf{f}_2 \ \ \mathbf{f}_3\right] \begin{bmatrix} \lambda_{i,u,1}^{k} & 0 & 0 \\ 0 & \lambda_{i,u,2}^{k} & 0 \\ 0 & 0 & \lambda_{i,u,3}^{k} \end{bmatrix} \left[\mathbf{f}_1 \ \ \mathbf{f}_2 \ \ \mathbf{f}_3\right]^{H}, \quad (9)$$

while $\bar{\mathbf{H}}_{k,u}^{\mathrm{C}}$ in (8) is rewritten as

$$\bar{\mathbf{H}}_{k,u}^{\mathrm{C}} = \left[\mathbf{f}_1 \ \ \mathbf{f}_2 \ \ \mathbf{f}_3\right] \begin{bmatrix} \lambda_{k,u,1}^{\mathrm{C}} & 0 & 0 \\ 0 & \lambda_{i,u,2}^{\mathrm{C}} & 0 \\ 0 & 0 & \lambda_{i,u,3}^{\mathrm{C}} \end{bmatrix} \left[\mathbf{f}_1 \ \ \mathbf{f}_2 \ \ \mathbf{f}_3\right]^{H}, \quad (10)$$

where $\mathbf{f}_n$ is the n-th column of 3-point IDFT matrix, and $\lambda_{i,u,n}^{k}$ and $\lambda_{k,u,1}^{\mathrm{C}}$ are the n-th eigenvalues of $\bar{\mathbf{G}}_{i,u}^{k}$ and $\bar{\mathbf{H}}_{k,u}^{\mathrm{C}}$ associated with an eigenvector $\mathbf{f}_n$, respectively. Then the received signal vector $\bar{\mathbf{y}}_k$ is rewritten as

$$\begin{aligned}\bar{\mathbf{y}}_k &= \sum_{u=1}^{2} \bar{\mathbf{H}}_{k,u}\mathbf{f}_1 s_{k,u} + \sum_{i\neq k} \sum_{u=1}^{2} \bar{\mathbf{G}}_{i,u}^{k}\mathbf{f}_1 s_{i,u} + \bar{\mathbf{z}}_k \\ &= \sum_{u=1}^{2} \bar{\mathbf{H}}_{k,u}^{\mathrm{NC}}\mathbf{f}_1 s_{k,u} + \left\{ \sum_{u=1}^{2} \lambda_{k,u,1}^{\mathrm{C}} s_{k,u} + \sum_{i\neq k} \sum_{u=1}^{2} \lambda_{i,u,1}^{k} s_{i,u} \right\} \mathbf{f}_1 + \bar{\mathbf{z}}_k.\end{aligned} \quad (11)$$

As seen in (11), all ICI signals are now aligned to the same direction, $\mathbf{f}_1$. Therefore, these ICI signals can be eliminated by multiplying an orthogonal projection matrix $\mathbf{W} = [\mathbf{f}_2, \mathbf{f}_3]^H$ to $\bar{\mathbf{y}}_k$. The effective received signal after the ICI cancellation is obtained as

$$\begin{aligned}\tilde{\mathbf{y}}_k &= \mathbf{W}\bar{\mathbf{y}}_k = \sum_{u=1}^{2} \mathbf{W}\bar{\mathbf{H}}_{k,u}^{\mathrm{NC}}\mathbf{f}_1 s_{k,u} + \mathbf{W}\bar{\mathbf{z}}_k \\ &= \underbrace{\begin{bmatrix} \mathbf{f}_2^H \bar{\mathbf{H}}_{k,1}^{\mathrm{NC}}\mathbf{f}_1 & \mathbf{f}_2^H \bar{\mathbf{H}}_{k,2}^{\mathrm{NC}}\mathbf{f}_1 \\ \mathbf{f}_3^H \bar{\mathbf{H}}_{k,1}^{\mathrm{NC}}\mathbf{f}_1 & \mathbf{f}_3^H \bar{\mathbf{H}}_{k,2}^{\mathrm{NC}}\mathbf{f}_1 \end{bmatrix}}_{\tilde{\mathbf{H}}_k} \underbrace{\begin{bmatrix} s_{k,1} \\ s_{k,2} \end{bmatrix}}_{\mathbf{s}_k} + \underbrace{\begin{bmatrix} \mathbf{f}_2^H \bar{\mathbf{z}}_k \\ \mathbf{f}_3^H \bar{\mathbf{z}}_k \end{bmatrix}}_{\tilde{\mathbf{z}}_k}.\end{aligned} \quad (12)$$

The above effective signal only contains the desired signals from the users in the own cell, where the effective channel matrix $\tilde{\mathbf{H}}_k$ in (12) is decomposed as

$$\tilde{\mathbf{H}}_k = \frac{1}{3} \begin{bmatrix} \frac{1}{2} + \frac{\sqrt{3}}{2}j & 1 \\ \frac{1}{2} - \frac{\sqrt{3}}{2}j & 1 \end{bmatrix} \begin{bmatrix} h_{k,1}[2] & h_{k,2}[2] \\ h_{k,1}[3] & h_{k,2}[3] \end{bmatrix}. \quad (13)$$

Because $h_{k,u}[\ell]$ is independently drawn from a continuous distribution, the rank of $\tilde{\mathbf{H}}_k$ is two with probability one. As a result, the data symbols sent from the two users, $s_{k,1}$ and $s_{k,2}$, are decodable at the k-th BS, provided that local CSIR is available with sufficiently large SNR. Since four time slots are used to deliver $2K$ independent data symbols, the sum-DoF is given by $d_{\Sigma} = \frac{K}{2}$. Note that in this example, inter-block interference caused by multiple block transmissions is ignored as it can be mitigated by using a successive-interference-cancellation technique; this will be explained with more details in the next section. The proposed interference management method described in this example is illustrated in Fig. 2.

Remark 1 (The Design of Precoder and Combiner): In Example 1, one important observation is that the proposed interference management method does not require instantaneous CSIT in the design of precoder and combiner. The underlying fact is that all channel matrices of ICI links become circulant at the BS, after applying a linear combining matrix that depends only on the number of CIR taps. Therefore,

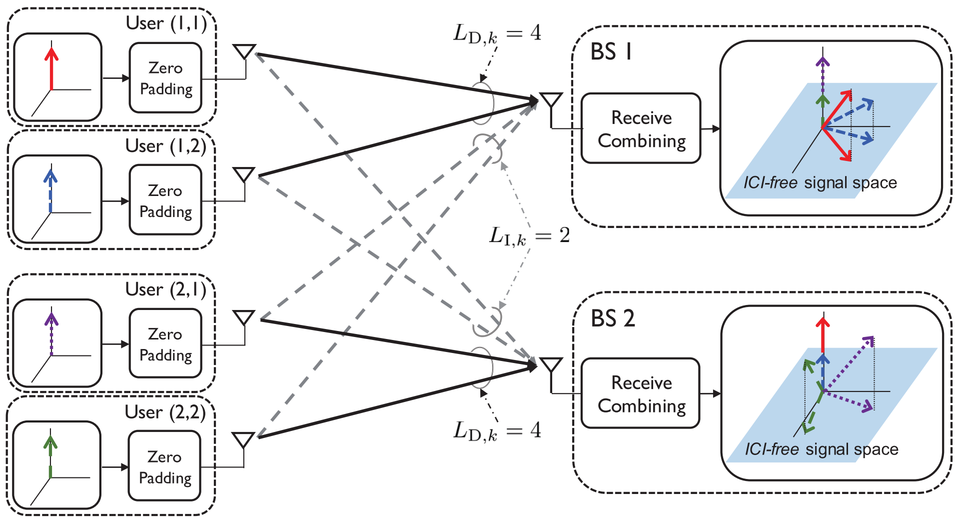

Fig. 2. A conceptual illustration of the proposed interference management method for the two-cell MAC with ISI when two users exist per cell.

to align ICI signals, the common precoder is only required to be determined as the combination of the eigenvectors of the circulant matrix (i.e., a column vector of the IDFT matrix) regardless of channel realizations. Similarly, to cancel the ICI signals at the BS, it only requires to multiply an orthogonal projection matrix $\mathbf{W}$ as a receive combiner, which is solely determined by the precoder.

IV. Main Result

In this section, we establish the main result of this paper by generalizing the blind interference management method introduced in Section III.

Theorem 1: Consider a K-cell MAC with ISI and constant channel coefficients. Let $L_{\mathrm{I}} = \max_k L_{\mathrm{I},k}$, $\Delta_k = (L_{\mathrm{D},k} - L_{\mathrm{I},k})^+$, and $\Delta_{\mathrm{D}} = \max_k \Delta_k$. The achievable sum-DoF of this channel without instantaneous CSIT is

$$d_{\Sigma}^{\mathrm{MAC}} = \max\left\{\sum_{k=1}^{K} \frac{\min\{U_k, \Delta_k\} M_k}{\max\{\Delta_{\mathrm{D}} + M_{\mathrm{D}}, L_{\mathrm{I}} - 1\} + L_{\mathrm{I}} - 1}, 1\right\}, \tag{14}$$

where $M_k = \max\left\{\left\lfloor \frac{\Delta_k}{U_k} \right\rfloor, 1\right\}$ and $M_{\mathrm{D}} = \max_k M_k$.

Proof: In this proof, we only focus on the case that

$$\sum_{k=1}^{K} \frac{\min\{U_k, \Delta_k\} M_k}{\max\{\Delta_{\mathrm{D}} + M_{\mathrm{D}}, L_{\mathrm{I}} - 1\} + L_{\mathrm{I}} - 1} > 1, \tag{15}$$

because otherwise, the trivial sum-DoF of one is achievable by using time-division multiple access (TDMA) among the BSs with OFDMA in each cell.

A. Block Transmission Strategy

We start the proof by presenting a block transmission strategy that consists of B subblock transmissions.

During the block transmission in cell k, only $U'_k \leq U_k$ users are active and each active user sends M_k data symbols for each subblock. By defining $\Delta_k = (L_{\mathrm{D},k} - L_{\mathrm{I},k})^+$ for $k \in \mathcal{K}$, we determine the number of active users as $U'_k = \min\{U_k, \Delta_k\}$ and the number of data streams per user as $M_k = \max\left\{\left\lfloor \frac{\Delta_k}{U_k} \right\rfloor, 1\right\}$. Each subblock transmission consists of $\bar{N} = N + L_{\mathrm{I}} - 1$ time slots, where $N = \max\{\Delta_{\mathrm{D}} + M_{\mathrm{D}}, L_{\mathrm{I}} - 1\}$, $\Delta_{\mathrm{D}} = \max_k \Delta_k$, and $M_{\mathrm{D}} = \max_k M_k$. After transmitting B subblocks, we append $L_{\mathrm{D}} - L_{\mathrm{I}}$ zeros at the end of the transmission block, to avoid inter-block interference between two subsequent block transmissions. Therefore, the total number of time slots needed for a single block transmission is $T = B\bar{N} + L_{\mathrm{D}} - L_{\mathrm{I}}$. Note that the duration of the subblock transmission is set to be shorter than that used in [34]. In fact, this reduced duration is a major source that yields the sum-DoF gain compared to the original method in [34]. In the sequel, we will provide a lemma which shows that the decodability of all data symbols at the BS is preserved even with the reduction in the transmission duration.

During the subblock transmission, each user (k, u) transmits M_k data symbols using a DFT-based precoding. Let $\mathbf{s}_{k,u}^b = [s_{k,u,1}^b, s_{k,u,2}^b, \cdots, s_{k,u,M_k}^b] \in \mathbb{C}^{M_k}$ be the data symbol vector of user (k, u) transmitted during the b-th subblock transmission. User (k, u) uses a precoding matrix $\mathbf{F}_k = [\mathbf{f}_1, \mathbf{f}_2, \ldots, \mathbf{f}_{M_k}] \in \mathbb{C}^{N \times M_k}$ to send the data symbol vector $\mathbf{s}_{k,u}^b$, so the precoded data symbol vector, namely $\bar{\mathbf{x}}_{k,u}^b \in \mathbb{C}^N$, is given by

$$\begin{aligned}\bar{\mathbf{x}}_{k,u}^b &= \left[x_{k,u}[(b-1)\bar{N}+1], \cdots, x_{k,u}[(b-1)\bar{N}+N]\right]^\top \\ &= \mathbf{F}_k \mathbf{s}_{k,u}^b = \sum_{m=1}^{M_k} \mathbf{f}_m s_{k,u,m}^b,\end{aligned} \tag{16}$$

for $u \in \mathcal{U}_k$, $k \in \mathcal{K}$, and $b \in \{1, 2, \ldots, B\}$. At the end of $\bar{\mathbf{x}}_{k,u}^b$, $L_{\mathrm{I}} - 1$ zeros are appended, so that the transmitted signal vector is generated as

$$\mathbf{x}_{k,u}^b = \Big[\bar{\mathbf{x}}_{k,u}^b, \underbrace{0, \ldots, 0}_{L_{\mathrm{I}}-1}\Big]^\top \in \mathbb{C}^{\bar{N}}. \tag{17}$$

Using the above strategy, the signal vector of user (k, u) transmitted during a single block transmission is

$$\mathbf{x}_{k,u} = \left[\left(\mathbf{x}_{k,u}^1\right)^\top, \left(\mathbf{x}_{k,u}^2\right)^\top, \cdots, \left(\mathbf{x}_{k,u}^B\right)^\top, \underbrace{0,\ldots,0}_{L_{\mathrm{D}}-L_{\mathrm{I}}} \right]^\top. \tag{18}$$

B. Received Signal Representation

We specify received signals at the BS during each subblock transmission. From (1), the received signal of the k-th BS at time slot n of the b-th subblock transmission is represented as

$$\begin{aligned} y_k[(b-1)\bar{N}+n] &= \sum_{u=1}^{U_k'} \sum_{\ell=0}^{L_{\mathrm{D},k}-1} h_{k,u}[\ell] x_{k,u}[(b-1)\bar{N}+n-\ell] \\ &\quad + \sum_{i\neq k} \sum_{u=1}^{U_i'} \sum_{\ell=0}^{L_{\mathrm{I},k}-1} g_{i,u}^k[\ell] x_{i,u}[(b-1)\bar{N}+n-\ell] \\ &\quad + z_k[(b-1)\bar{N}+n], \end{aligned} \tag{19}$$

for $n \in \{1,2,\ldots,\bar{N}\}$ and $b \in \{1,2,\ldots,B\}$. By collecting all received signals for each subblock transmission, the received signal vector of the k-th BS at the b-th subblock transmission is

$$\mathbf{y}_k^b = \left[y_k[(b-1)\bar{N}+1], \cdots, y_k[b\bar{N}] \right]^\top \in \mathbb{C}^{\bar{N}}. \tag{20}$$

Similarly, the noise vector of the k-th BS at the b-th subblock transmission is

$$\mathbf{z}_k^b = \left[z_k[(b-1)\bar{N}+1], \cdots, z_k[b\bar{N}] \right]^\top \in \mathbb{C}^{\bar{N}}. \tag{21}$$

We use a receive combining matrix, namely $\mathbf{D}_k \in \{1,0\}^{N\times\bar{N}}$, to combine the received signal vector in (20). The receive combining matrix is defined as

$$\mathbf{D}_k = \begin{bmatrix} \mathbf{I}_N & \begin{matrix} \mathbf{I}_{L_{\mathrm{I},k}-1} \\ \mathbf{0}_{(N-L_{\mathrm{I},k}+1)\times(L_{\mathrm{I},k}-1)} \end{matrix} & \mathbf{0}_{N\times(L_{\mathrm{I}}-L_{\mathrm{I},k})} \end{bmatrix}. \tag{22}$$

Then the combined received signal at the k-th BS is obtained as

$$\begin{aligned} \bar{\mathbf{y}}_k^b = \mathbf{D}_k \mathbf{y}_k^b &= \sum_{u=1}^{U_k'} \bar{\mathbf{H}}_{k,u}^k \bar{\mathbf{x}}_{k,u}^b + \sum_{i=1,i\neq k}^{K} \sum_{u=1}^{U_i'} \bar{\mathbf{H}}_{i,u}^k \bar{\mathbf{x}}_{i,u}^b + \bar{\mathbf{z}}_k^b \\ &= \sum_{u=1}^{U_k'} \bar{\mathbf{H}}_{k,u}^k \mathbf{F}_k \mathbf{s}_{k,u}^b + \sum_{i=1,i\neq k}^{K} \sum_{u=1}^{U_i'} \bar{\mathbf{H}}_{i,u}^k \mathbf{F}_k \mathbf{s}_{i,u}^b + \bar{\mathbf{z}}_k^b, \end{aligned} \tag{23}$$

where $\bar{\mathbf{z}}_k^b = \mathbf{D}_k \mathbf{z}_k^b$. For the ease of exposition, we define $\mathrm{Circ}(\mathbf{c})$ as an n by n circulant matrix when its first column is $\mathbf{c} \in \mathbb{C}^n$. Using this notation, the channel matrix of the ICI link between user (i,u) and the k-th BS for $i \neq k$ is represented as

$$\bar{\mathbf{G}}_{i,u}^k = \mathrm{Circ}\left(\left[g_{i,u}^k[0], \cdots, g_{i,u}^k[L_{\mathrm{I},k}-1], \underbrace{0,\ldots,0}_{N-L_{\mathrm{I},k}} \right]\right). \tag{24}$$

Whereas, the channel matrix of the desired link between user (k,u) and the k-th BS is decomposed into two matrices:

$$\bar{\mathbf{H}}_{k,u} = \bar{\mathbf{H}}_{k,u}^{\mathrm{C}} + \bar{\mathbf{H}}_{k,u}^{\mathrm{NC}}, \tag{25}$$

where

$$\bar{\mathbf{H}}_{k,u}^{\mathrm{C}} = \mathrm{Circ}\left(\left[h_{k,u}[0], \cdots, h_{k,u}[N_{k,u}'-1], \underbrace{0,\ldots,0}_{(N-L_{\mathrm{D},k})^+} \right]\right), \tag{26}$$

with $N_k' = \min\{L_{\mathrm{D},k}, N\}$, and $\bar{\mathbf{H}}_{k,u}^{\mathrm{NC}}$ has the form of

$$\bar{\mathbf{H}}_{k,u}^{\mathrm{NC}} = \begin{bmatrix} \bar{\mathbf{H}}_{k,u}^{\mathrm{low}} & \mathbf{0}_{(L_{\mathrm{I},k}-1)\times(N-L_{\mathrm{I},k}+1)} \\ \mathbf{0}_{(N-L_{\mathrm{I},k}+1)\times(L_{\mathrm{I},k}-1)} & -\bar{\mathbf{H}}_{k,u}^{\mathrm{upp}} \end{bmatrix}. \tag{27}$$

In (27), $\bar{\mathbf{H}}_{k,u}^{\mathrm{upp}} \in \mathbb{C}^{(N-L_{\mathrm{I},k}+1)\times(N-L_{\mathrm{I},k}+1)}$ and $\bar{\mathbf{H}}_{k,u}^{\mathrm{low}} \in \mathbb{C}^{(L_{\mathrm{I},k}-1)\times(L_{\mathrm{I},k}-1)}$ are upper and lower toeplitz matrices defined in (28) (see the top of the next page). Note that when $N \geq L_{\mathrm{D},k}$, $\bar{\mathbf{H}}_{k,u}^{\mathrm{low}} = \mathbf{0}_{(L_{\mathrm{I},k}-1)\times(L_{\mathrm{I},k}-1)}$ by the definition of (28). Plugging (25) into (23), we have

$$\bar{\mathbf{y}}_k^b = \sum_{u=1}^{U_k'} \left(\bar{\mathbf{H}}_{k,u}^{\mathrm{NC}} + \bar{\mathbf{H}}_{k,u}^{\mathrm{C}}\right) \mathbf{F}_k \mathbf{s}_{k,u}^b + \sum_{i\neq k} \sum_{u=1}^{U_i'} \bar{\mathbf{G}}_{i,u}^k \mathbf{F}_k \mathbf{s}_{i,u}^b + \bar{\mathbf{z}}_k^b, \tag{29}$$

for $k \in \mathcal{K}$ and $b \in \{1,2,\ldots,B\}$. As seen in (24) and (29), the channel matrices of ICI links are circulant matrices, while the channel matrices of desired links are the superposition of circulant and non-circulant matrices. Using the above transmission/reception strategy, we create *the relativity in channel matrix structure between desired and ICI links.*

C. Inter-Cell-Interference Cancellation

We explain a ICI cancellation method that harnesses the matrix structural relativity between desired and ICI links. We start by providing a lemma that is essential for our proof.

Lemma 1: A circulant matrix $\mathbf{C} \in \mathbb{C}^{n\times n}$ is decomposed as

$$\mathbf{C} = \mathbf{F}\boldsymbol{\Lambda}\mathbf{F}^H, \tag{30}$$

where $\mathbf{F} = [\mathbf{f}_1, \mathbf{f}_2, \ldots, \mathbf{f}_n] \in \mathbb{C}^{n\times n}$ is the n-point IDFT matrix whose k-th column vector is defined as $\mathbf{f}_k = \frac{1}{\sqrt{n}}\left[1, \omega^{k-1}, \omega^{2(k-1)}, \ldots, \omega^{(n-1)(k-1)}\right]^H$, with $\omega = \exp\left(-j\frac{2\pi}{n}\right)$ for $k \in \{1,2,\ldots,n\}$. ■

Proof: See [35].

As seen in (24) and (29), the channel matrices of ICI links are circulant. Therefore, from Lemma 1, the columns of the precoding matrix $\mathbf{F}_k$ are the eigenvectors of these ICI channel matrices. This implies that all the ICI signals in (29) are aligned in the subspace formed by $\mathbf{F}_k$, i.e., $\mathrm{span}\left(\bar{\mathbf{G}}_{i,u}^k \mathbf{F}_k\right) = \mathrm{span}(\mathbf{F}_k)$ for $i \neq k$ and $i,k \in \mathcal{K}$. As a result, we can eliminate all the ICI signals by projecting $\bar{\mathbf{y}}_k^b$ in (29) onto the orthogonal subspace of $\mathbf{F}_k$. To this end, we use a receive combining matrix defined as $\mathbf{W} = \left[\mathbf{f}_{M_{\mathrm{D}}+1}, \cdots, \mathbf{f}_N\right]^H \in \mathbb{C}^{(N-M_{\mathrm{D}})\times N}$. Then the effective received signal vector of the k-th BS during the b-th subblock transmission, namely $\tilde{\mathbf{y}}_k^b \in \mathbb{C}^{N-M_{\mathrm{D}}}$, is given by

$$\tilde{\mathbf{y}}_k^b = \mathbf{W}\bar{\mathbf{y}}_k^b = \sum_{u=1}^{U_k'} \mathbf{W}\bar{\mathbf{H}}_{k,u}^{\mathrm{NC}} \mathbf{F}_k \mathbf{s}_{k,u}^b + \mathbf{W}\bar{\mathbf{z}}_k^b, \tag{31}$$

for $k \in \mathcal{K}$ and $b \in \{1,2,\ldots,B\}$, Now, the effective received signal vector in (31) only contains the transmitted signals from the associating users without ICI.

$$\bar{\mathbf{H}}_{k,u}^{\mathrm{upp}} = \begin{bmatrix} 0 & \cdots & 0 & h_{k,u}[N_k'-1] & \cdots & h_{k,u}[L_{\mathrm{I},k}] \\ \vdots & 0 & & 0 & \ddots & \vdots \\ \vdots & & \ddots & & \ddots & h_{k,u}[N_k'-1] \\ \vdots & & & \ddots & & 0 \\ \vdots & & & & \ddots & \vdots \\ 0 & 0 & \cdots & \cdots & \cdots & 0 \end{bmatrix}$$

and

$$\bar{\mathbf{H}}_{k,u}^{\mathrm{low}} = \begin{bmatrix} h_{k,u}[N_k'] & 0 & \cdots & \cdots & \cdots & 0 \\ \vdots & h_{k,u}[N_k'] & 0 & & & \vdots \\ h_{k,u}[L_{\mathrm{D},k}-1] & & \ddots & \ddots & & \vdots \\ 0 & \ddots & & \ddots & \ddots & \vdots \\ \vdots & \ddots & \ddots & & \ddots & 0 \\ 0 & \cdots & 0 & h_{k,u}[L_{\mathrm{D},k}-1] & \cdots & h_{k,u}[N_k'] \end{bmatrix}. \tag{28}$$

D. Decodability of Subblock Data

To accomplish our proof, we show the decodability of the data symbols in each subblock transmission. First, we find the equivalent representation of (31) in which an effective channel is represented as a MIMO channel; then show that this effective channel matrix has full rank.

To simplify the expression in (31), we define an effective channel matrix $\tilde{\mathbf{H}}_k \in \mathbb{C}^{(N-M_{\mathrm{D}})\times U_k' M_k}$ as follows:

$$\tilde{\mathbf{H}}_k = \left[\mathbf{W}\bar{\mathbf{H}}_{k,1}^{\mathrm{NC}}\mathbf{F}_k,\ \mathbf{W}\bar{\mathbf{H}}_{k,2}^{\mathrm{NC}}\mathbf{F}_k,\ \cdots,\ \mathbf{W}\bar{\mathbf{H}}_{k,U_k'}^{\mathrm{NC}}\mathbf{F}_k \right]. \tag{32}$$

Then the effective received signal vector in (31) simplifies to

$$\tilde{\mathbf{y}}_k^b = \tilde{\mathbf{H}}_k \mathbf{s}_k^b + \tilde{\mathbf{z}}_k^b, \tag{33}$$

where $\mathbf{s}_k^b = \left[\mathbf{s}_{k,1}^b, \mathbf{s}_{k,2}^b, \cdots, \mathbf{s}_{k,U_k'}^b\right]^\top \in \mathbb{C}^{U_k' M_k}$ is the total data symbol vector received at the k-th BS during the b-th subblock transmission, and $\tilde{\mathbf{z}}_k^b = \mathbf{W}\bar{\mathbf{z}}_k^b \in \mathbb{C}^{N-M_{\mathrm{D}}}$ is an effective noise vector. Note that the distribution of $\tilde{\mathbf{z}}_k^b$ is invariant with $\bar{\mathbf{z}}_k^b$ because $\mathbf{W}$ is a unitary transformation matrix. Since the expression in (33) is equivalent to a simple MIMO system, to guarantee the decodability of $\mathbf{s}_k^b$ in (33), we only need to show whether the rank of $\tilde{\mathbf{H}}_k$ equals $U_k' M_k$ which is the number of data symbols sent by the users in cell k. The following lemma essentially shows our decodability result.

Lemma 2: The rank of $\tilde{\mathbf{H}}_k$ defined in (32) is

$$\mathrm{rank}\left(\tilde{\mathbf{H}}_k\right) = U_k' M_k, \quad \text{for} \quad k \in \mathcal{K}. \tag{34}$$

Proof: See Appendix. ■

Lemma 2 implies that for sufficiently large SNR, all $U_k' M_k$ data symbols in $\mathbf{s}_k^b$ can be reliably decoded. For example, we can apply MLD or ZFD methods to detect $\mathbf{s}_k^b$ from (33). Note that the proof technique of Lemma 2 is a generalization of that given in [34], as it requires additional linear algebraic techniques along with the property of the DFT matrix to exploit channel diversity provided by the transmission of multiple users.

E. Inter-Subblock-Interference Cancellation

We have shown that $U_k' M_k$ data symbols are decodable for each subblock transmission, by assuming that there is no inter-subblock interference (ISBI). Unfortunately, ISBI between two subsequent subblocks is unpreventable because of the delayed signal from the previous subblock transmission is observed at the receiver. Thus, a cancellation method of ISBI is needed for multiple subblock transmissions.

After discarding $L_{\mathrm{D}}-L_{\mathrm{I}}$ zeros at the end of the transmission block, we concatenate the received vectors from all subblock transmissions. Because the channel coefficients are constant during each block transmission, when ignoring noise, the total input-output relationship during an entire block transmission is

$$\begin{bmatrix} \tilde{\mathbf{y}}_k^1 \\ \tilde{\mathbf{y}}_k^2 \\ \vdots \\ \tilde{\mathbf{y}}_k^B \end{bmatrix} = \begin{bmatrix} \tilde{\mathbf{H}}_k & \mathbf{0}^{\mathrm{sub}} & \cdots & \cdots & \mathbf{0}^{\mathrm{sub}} \\ \tilde{\mathbf{H}}_k^{\mathrm{sub}} & \tilde{\mathbf{H}}_k & \ddots & \ddots & \vdots \\ \mathbf{0}^{\mathrm{sub}} & \tilde{\mathbf{H}}_k^{\mathrm{sub}} & \ddots & \ddots & \vdots \\ \vdots & \ddots & \ddots & \tilde{\mathbf{H}}_k & \mathbf{0}^{\mathrm{sub}} \\ \mathbf{0}^{\mathrm{sub}} & \cdots & \mathbf{0}^{\mathrm{sub}} & \tilde{\mathbf{H}}_k^{\mathrm{sub}} & \tilde{\mathbf{H}}_k \end{bmatrix} \begin{bmatrix} \mathbf{s}_k^1 \\ \mathbf{s}_k^2 \\ \vdots \\ \mathbf{s}_k^B \end{bmatrix}, \tag{35}$$

where $\tilde{\mathbf{H}}_k^{\mathrm{sub}} \in \mathbb{C}^{(N-M_{\mathrm{D}})\times U_k' M_k}$ is the effective channel matrix for ISBI at the k-th BS, and $\mathbf{0}^{\mathrm{sub}} = \mathbf{0}_{(N-M_{\mathrm{D}})\times U_k' M_k}$. By the definition, one can easily verify that $\tilde{\mathbf{H}}_k^{\mathrm{sub}}$ is given by

$$\tilde{\mathbf{H}}_k^{\mathrm{sub}} = \left[\mathbf{W}\bar{\mathbf{H}}_{k,1}^{\mathrm{sub}}\mathbf{F}_k, \mathbf{W}\bar{\mathbf{H}}_{k,2}^{\mathrm{sub}}\mathbf{F}_k, \cdots, \mathbf{W}\bar{\mathbf{H}}_{k,U_k'}^{\mathrm{sub}}\mathbf{F}_k \right]. \tag{36}$$

where $\bar{\mathbf{H}}_{k,u}^{\mathrm{sub}} \in \mathbb{C}^{N\times N}$ is

$$\bar{\mathbf{H}}_{k,u}^{\mathrm{sub}} = \begin{bmatrix} \mathbf{0}_{(N-L_{\mathrm{I}}+1)\times(L_{\mathrm{I}}-1)} & \bar{\mathbf{H}}_{k,u}^{\mathrm{upp}}\Big|_{N_k'=L_{\mathrm{D},k}} \\ \mathbf{0}_{(L_{\mathrm{I}}-1)\times(L_{\mathrm{I}}-1)} & \mathbf{0}_{(L_{\mathrm{I}}-1)\times(N-L_{\mathrm{I}}+1)} \end{bmatrix}. \tag{37}$$

At the first subblock transmission, there is no ISBI, i.e., $\tilde{\mathbf{y}}_k^1 = \tilde{\mathbf{H}}_k\mathbf{s}_k^1 + \tilde{\mathbf{z}}_k^1$, so the symbol vector $\mathbf{s}_k^1$ is reliably decodable for a sufficiently large SNR value. At the b-th subblock transmission for $b \geq 2$, under the premise that $\mathbf{s}_k^{b-1}$ is reliably decodable, it is possible to decode $\mathbf{s}_k^b$ by subtracting the effect of $\mathbf{s}_k^{b-1}$ from the received signal $\tilde{\mathbf{y}}_k^b$ as follows:

$$\tilde{\mathbf{y}}_k^b - \tilde{\mathbf{H}}_k^{\text{sub}}\mathbf{s}_k^{b-1} = \tilde{\mathbf{H}}_k\mathbf{s}_k^b + \tilde{\mathbf{z}}_k^b. \tag{38}$$

One practical concern with this successive interference cancellation method is that, when SNR is low, it may suffer from error propagation. Nevertheless, this approach is sufficient to show the DoF result in the high SNR regime.

F. Achievable Sum-DoF Calculation

Applying the above ISBI cancellation strategy over B subblocks recursively, the k-th BS is capable of decoding B data symbol vectors $\mathbf{s}_k^1, \mathbf{s}_k^2, \ldots, \mathbf{s}_k^B$, with $T = B\bar{N} + L_{\text{D}} - 1$ time slots. By the definition in (2), the achievable DoF of the k-th BS when taking B to infinity is given by

$$d_k = \lim_{B\to\infty} \frac{BU_k' M_k}{B(N+L_{\text{I}}-1)+L_{\text{D}}-L_{\text{I}}} = \frac{U_k' M_k}{N+L_{\text{I}}-1}, \tag{39}$$

provided that the channel coefficients are constant during the coherence time. By plugging $N = \max\{\Delta_{\text{D}} + M_{\text{D}}, L_{\text{I}} - 1\}$ to (39), we arrive at the expression in Theorem 1. ∎

Theorem 1 shows the achievable sum-DoF when delay spreads are asymmetric for different cells, yet it is unwieldy to provide a clear intuition in the result. Therefore, we also present a corollary that simplifies Theorem 1 under the premise that the delay spreads are symmetric:

Corollary 1 (Achievable Sum-DoF For Symmetric Delay Spread): Consider a K-cell MAC with ISI and constant channel coefficients. If delay spreads of wireless channels for difference cells are symmetric, i.e., $L_{\text{D},k} = L_{\text{D}}$ and $L_{\text{I},k} = L_{\text{I}}$ for $k \in \mathcal{K}$, the achievable sum-DoF of the considered channel is

$$d_\Sigma^{\text{MAC}} = \left(1 - \frac{L_{\text{I}}}{L_{\text{D}}}\right) K \to K, \quad \text{as} \quad \frac{L_{\text{D}}}{L_{\text{I}}} \to \infty, \tag{40}$$

provided that the number of users per cell is larger than $L_{\text{D}} - L_{\text{I}}$ and $L_{\text{D}} \geq 2(L_{\text{I}} - 1)$.

Proof: Suppose that $L_{\text{D},k} = L_{\text{D}}$, $L_{\text{I},k} = L_{\text{I}}$, $U_k \geq \Delta_{\text{D}} = L_{\text{D}} - L_{\text{I}}$ for $k \in \mathcal{K}$, and $L_{\text{D}} \geq 2(L_{\text{I}} - 1)$. Applying these specific parameters to (14) yields the result in (40). ∎

Corollary 1 implies that *interference-free DoF per cell* is asymptotically achievable even without CSIT, as the ratio of the CIR length of desired links to that of ICI links approaches infinity with a sufficiently large number of users per cell. Note that when $\frac{L_{\text{D}}}{L_{\text{I}}}$ is finite, the achievable sum-DoF is strictly less than the interference-free sum-DoF of K, because $d_\Sigma^{\text{MAC}} = \left(1 - \frac{L_{\text{I}}}{L_{\text{D}}}\right) K < K$ for any $0 < \frac{L_{\text{D}}}{L_{\text{I}}} < \infty$.

When the ICI links have small delay spreads, the condition required to achieve K sum-DoF can be further relaxed. For example, if all ICI links are line-of-sight channels, i.e., $L_{\text{I}} = 1$, the equation in (40) becomes

$$d_\Sigma^{\text{MAC}} = \frac{L_{\text{D}} - 1}{L_{\text{D}}} K. \tag{41}$$

In this case, nearly K sum-DoF is achievable even when both the number of users and the number of CIR taps for desired links are not so large.

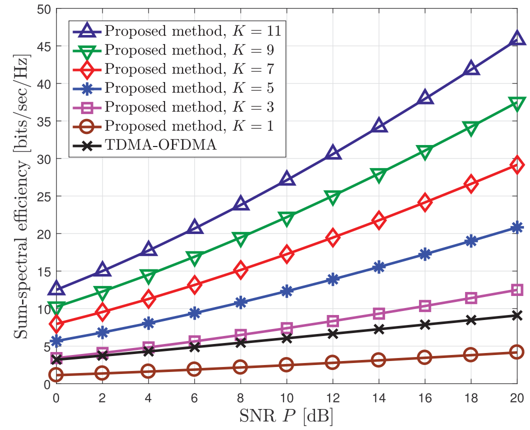

Fig. 3. Comparison of sum-spectral efficiency between TDMA-OFDMA and the proposed interference management method for different K. We set $B = 10$, $L_{\text{D},k} = 8$, $L_{\text{I},k} = 2$, and $U_k = 3$ for $k \in \mathcal{K}$. Each CIR tap is drawn from $\mathcal{CN}(0, 1)$.

With the proposed interference management method, it is also possible to characterize the achievable sum-spectral efficiency in a closed form, as given in the following Corollary:

Corollary 2 (Achievable Sum-Spectral Efficiency): Consider a K-cell MAC with ISI, each cell with U_k' active uplink users that transmit M_k data symbols respectively. Then the achievable sum-spectral efficiency of this channel without instantaneous CSIT is

$$\sum_{k=1}^{K} \frac{B}{B(N + L_{\text{I}} - 1) + L_{\text{D}} - L_{\text{I}}} \times \log_2 \left| \mathbf{I}_{N-M_{\text{D}}} + \frac{T\rho}{BM_k} \left(\mathbf{W}\mathbf{D}_k\mathbf{D}_k^H\mathbf{W}^H\right)^{-1} \tilde{\mathbf{H}}_k\tilde{\mathbf{H}}_k^H \right|, \tag{42}$$

where $\rho = \frac{P}{\sigma^2}$ is SNR.

Proof: Under the premise that each user uses the Gaussian signaling, the achievable rate at the k-th BS sent over $T = B(N + L_{\text{I}} - 1) + L_{\text{D}} - L_{\text{I}}$ time slots is computed as

$$R_k(P) = \frac{1}{T} \sum_{m=1}^{U_k' M_k} \sum_{b=1}^{B} \log_2 \left| \mathbf{I}_{N-M_{\text{D}}} + \left(\sigma^2 \mathbf{W}\mathbf{D}_k\mathbf{D}_k^H\mathbf{W}^H\right)^{-1} \times \tilde{\mathbf{H}}_k \mathbb{E}\left[\mathbf{s}_{k,u}^b (\mathbf{s}_{k,u}^b)^H\right] \tilde{\mathbf{H}}_k^H \right|, \tag{43}$$

from (38). Since $\mathbb{E}[|x_{k,u}[n]|^2] = P$ is assumed, a total power constraint for T time slots is given by $\sum_{b=1}^{B} \mathbb{E}[\|\mathbf{F}_k\mathbf{s}_{k,u}^b\|^2] = TP$. Therefore, $\mathbb{E}\left[\mathbf{s}_{k,u}^b (\mathbf{s}_{k,u}^b)^H\right] = \frac{TP}{BM_k}\mathbf{I}_{M_k}$ for all k, u, b. Applying this result to (43) yields the result in (42). ∎

Corollary 2 is useful to gauge the performance benefit of the proposed method in a low SNR regime. As a numerical example, Fig. 3 shows that the ergodic sum-spectral efficiency of the proposed interference management method increases linearly with K, so the proposed method outperforms TDMA-OFDMA in all SNR regimes when $K \geq 3$.

Remark 2 (Comparison With the Existing Work in [34]): The concept of the blind interference management with matrix structuring has originally been proposed in [34] for a K-user interference channel with ISI and no CSIT. The work in [34] has shown that the achievable sum-DoF of the considered interference channel is

$$d_{\Sigma}^{\mathrm{IC}} = K\frac{L_{\mathrm{D}}-L_{\mathrm{I}}}{\max\{2L_{\mathrm{D}}-L_{\mathrm{I}}-1, 2L_{\mathrm{I}}-1\}} \to \frac{K}{2} \quad \text{as} \quad \frac{L_{\mathrm{D}}}{L_{\mathrm{I}}} \to \infty, \tag{44}$$

when the delay spreads are symmetric for different users. Comparing (44) with (40) shows that the asymptotically achievable sum-DoF of the K-cell MAC is twice higher than that attained in the K-user interference channel even with ISI and no CSIT. This additional gain in sum-DoF is obtained from *channel diversity* in MAC, where independent channels are realized from different users.

Remark 3 (Comparison With a Time-Domain Approach): We conjecture that a *time-domain* method, in which all uplink users send their data symbols through cooperatively selected time-slots without any precoding, can achieve the same sum-DoF with the proposed method as claimed in Theorem 1. For instance, in Example 1, if all users transmit one data symbol using the first time slot and remains silent for the subsequent three time slots of every block of four time slots, the same sum-DoF of $\frac{K}{2}$ is achievable in this simple case. This time-domain method, however, is not straightforward and rather unwieldy when applying it into general ISI conditions. For example, when the ISI conditions vary over links, finding the optimal time slots that used for the uplink transmissions is not trivial, and it heavily depends on the ISI patterns. Therefore, it is still an open question how to characterize the sum-DoF of the multi-cell MAC using the time-domain method. Whereas, the proposed frequency-domain method is constructed in a systematic manner so that it is universally applicable regardless of ISI patterns. Despite this fact, as a future research, it would be interesting to investigate a more comprehensive comparison between two methods by characterizing not only the achievable sum-DoF, but also the spectral efficiency and the computational complexity.

V. Extension for Propagation Delay

In Section IV, the proposed interference management method has been presented under the assumption that the delay spread of the desired links is larger than that of ICI links and also that all CIR taps are non-zeros. These assumptions may not be hold in some wireless environments because they ignore the propagation delay which is likely to exist in the ICI links.

Motivated by the above fact, in this section, we extend the proposed interference management method for the use in two different cases: 1) $L_{\mathrm{D},k} > L_{\mathrm{I},k}$ and 2) $L_{\mathrm{D},k} \le L_{\mathrm{I},k}$, under the consideration of the propagation delay in the ICI links.

A. Propagation Delay With $L_{D,k} > L_{I,k}$

When a propagation delay exists in ICI links with $L_{\mathrm{D},k} > L_{\mathrm{I},k}$ as depicted in Fig. 4(b), the achievable sum-DoF of the proposed interference management method can be improved by exploiting ICI-free signals during the delay. In what follows, we demonstrate this improvement by using an illustrative example.

Example 2 (Propagation Delay With $L_{D,k} > L_{I,k}$): We consider a K-cell MAC with three users per cell when $L_{\mathrm{D},k} = L_{\mathrm{D}} = 5$ and $L_{\mathrm{I},k} = L_{\mathrm{I}} = 4$ for $k \in \mathcal{K}$. We denote $L_{\mathrm{I,d}}$ as the number of CIR taps during ICI delay offset, and also denote $L_{\mathrm{I}}^{\mathrm{eff}} = L_{\mathrm{I}} - L_{\mathrm{I,d}}$ as the effective (actual) number of CIR taps for ICI links. With these notations, we consider a delayed-ICI case with $L_{\mathrm{I}}^{\mathrm{eff}} = 2$, i.e., $g_{i,u}^{k}[0] = g_{i,u}^{k}[1] = 0$ for $u \in \mathcal{U}_i$, $i \neq k$, and $i, k \in \mathcal{K}$. In Fig. V(b), we depict the considered scenario. In this scenario, we will show that each BS reliably decodes three data symbols with seven time slots, i.e., $d_{\Sigma} = \frac{3K}{5}$, by using the proposed method in Section IV with a proper modification.

Applying the transmission strategy of the proposed interference management method, user (k,u) uses the first column of the 2-point IDFT matrix to convey one data symbol, i.e., $\bar{\mathbf{x}}_{k,u} = \mathbf{f}_1 s_{k,u} \in \mathbb{C}^2$, where $\mathbf{f}_n$ is the n-th column of the 2-point IDFT matrix and $s_{k,u}$ is the data symbol sent by user (k,u). Note that the size of the IDFT matrix chosen in this example is different from that chosen in Section IV. Then the received signal vector at the k-th BS during five time slots is given as

$$\underbrace{\begin{bmatrix} y_k[1] \\ y_k[2] \\ y_k[3] \\ y_k[4] \\ y_k[5] \end{bmatrix}}_{\bar{\mathbf{y}}_k} = \sum_{u=1}^{3} \begin{bmatrix} h_{k,u}[0] & 0 \\ h_{k,u}[1] & h_{k,u}[0] \\ h_{k,u}[2] & h_{k,u}[1] \\ h_{k,u}[3] & h_{k,u}[2] \\ h_{k,u}[4] & h_{k,u}[3] \end{bmatrix} \begin{bmatrix} x_{k,u}[1] \\ x_{k,u}[2] \end{bmatrix}$$
$$+ \sum_{i\neq k}\sum_{u=1}^{3} \begin{bmatrix} 0 & 0 \\ 0 & 0 \\ g_{i,u}^{k}[2] & 0 \\ g_{i,u}^{k}[3] & g_{i,u}^{k}[2] \\ 0 & g_{i,u}^{k}[3] \end{bmatrix} \begin{bmatrix} x_{i,u}[1] \\ x_{i,u}[2] \end{bmatrix} + \underbrace{\begin{bmatrix} z_k[1] \\ z_k[2] \\ z_k[3] \\ z_k[4] \\ z_k[5] \end{bmatrix}}_{\bar{\mathbf{z}}_k}. \tag{45}$$

It can be seen in (45) that the received signal vector is divided into two types of signals: *ICI-free* and *ICI-corrupted* signals. In (45), the first two received signals ($y_k[1]$ and $y_k[2]$) correspond to ICI-free signals, while the remaining three received signals correspond to ICI-corrupted signals. Our goal is to harness these ICI-free signals to increase the rank of the effective channel matrix $\tilde{\mathbf{H}}_k$. This can be achieved by choosing a proper receive combining matrix: In this case, the proper combining matrix is

$$\mathbf{W} = \begin{bmatrix} \mathbf{I}_2 & \mathbf{0}_{2\times 3} \\ \mathbf{0}_{1\times 2} & \mathbf{f}_2^H \mathbf{D} \end{bmatrix}, \quad \text{where } \mathbf{D} = \begin{bmatrix} 1 & 0 & 1 \\ 0 & 1 & 0 \end{bmatrix}. \tag{46}$$

By applying $\mathbf{W}$ in (46) to the received signal vector in (45), the effective received signal at the k-th BS is represented as

$$\begin{aligned} \tilde{\mathbf{y}}_k &= \mathbf{W}\bar{\mathbf{y}}_k \\ &= \sum_{u=1}^{3} \begin{bmatrix} \hat{\mathbf{H}}_{k,u} \\ \mathbf{f}_2^H \bar{\mathbf{H}}_{k,u} \end{bmatrix} \mathbf{f}_1 \; s_{k,u} + \sum_{i\neq k}\sum_{u=1}^{3} \begin{bmatrix} \mathbf{0}_{2\times 2} \\ \mathbf{f}_2^H \bar{\mathbf{G}}_{i,u}^{k} \end{bmatrix} \mathbf{f}_1 s_{i,u} + \mathbf{W}\bar{\mathbf{z}}_k, \end{aligned} \tag{47}$$

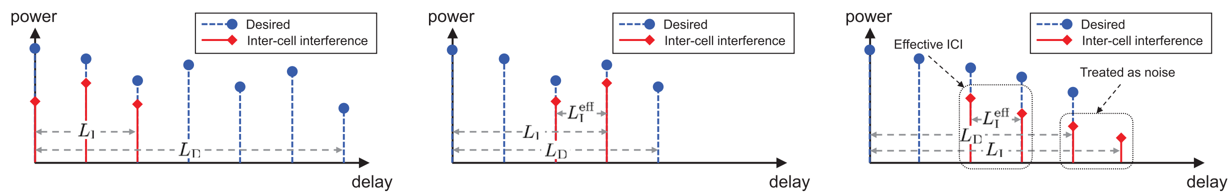

(a) $L_\mathrm{D} > L_\mathrm{I}$ without propagation delay (b) $L_\mathrm{D} > L_\mathrm{I}$ with propagation delay (c) $L_\mathrm{D} \le L_\mathrm{I}$ with propagation delay

Fig. 4. Three possible power-delay profiles of the channels with and without propagation delay.

where

$$\hat{\mathbf{H}}_{k,u} = \begin{bmatrix} h_{k,u}[0] & 0 \\ h_{k,u}[1] & h_{k,u}[0] \end{bmatrix},$$

$$\bar{\mathbf{H}}_{k,u} = \underbrace{\begin{bmatrix} h_{k,u}[2] & h_{k,u}[3] \\ h_{k,u}[3] & h_{k,u}[2] \end{bmatrix}}_{\bar{\mathbf{H}}^{\mathrm{C}}_{k,u}} + \underbrace{\begin{bmatrix} h_{k,u}[4] & h_{k,u}[1] \\ 0 & 0 \end{bmatrix}}_{\bar{\mathbf{H}}^{\mathrm{NC}}_{k,u}},$$

$$\bar{\mathbf{G}}^{k}_{i,u} = \begin{bmatrix} h^{k}_{i,u}[2] & h^{k}_{i,u}[3] \\ h^{k}_{i,u}[3] & h^{k}_{i,u}[2] \end{bmatrix}.$$

Because $\bar{\mathbf{H}}^{\mathrm{C}}_{k,u}$ and $\bar{\mathbf{G}}^{k}_{i,u}$ are circulant matrices, the effective received signal in (47) is rewritten as

$$\begin{aligned}\tilde{\mathbf{y}}_k &= \sum_{u=1}^{3} \begin{bmatrix} \hat{\mathbf{H}}_{k,u}\mathbf{f}_1 \\ \mathbf{f}_2^H \bar{\mathbf{H}}^{\mathrm{NC}}_{k,u}\mathbf{f}_1 \end{bmatrix} s_{k,u} + \mathbf{W}\bar{\mathbf{z}}_k \\ &= \underbrace{\begin{bmatrix} \hat{\mathbf{H}}_{k,1}\mathbf{f}_1 & \hat{\mathbf{H}}_{k,2}\mathbf{f}_1 & \hat{\mathbf{H}}_{k,3}\mathbf{f}_1 \\ \mathbf{f}_2^H \bar{\mathbf{H}}^{\mathrm{NC}}_{k,1}\mathbf{f}_1 & \mathbf{f}_2^H \bar{\mathbf{H}}^{\mathrm{NC}}_{k,2}\mathbf{f}_1 & \mathbf{f}_2^H \bar{\mathbf{H}}^{\mathrm{NC}}_{k,3}\mathbf{f}_1 \end{bmatrix}}_{\tilde{\mathbf{H}}_k} \underbrace{\begin{bmatrix} s_{k,1} \\ s_{k,2} \\ s_{k,3} \end{bmatrix}}_{\mathbf{s}_k} + \mathbf{W}\bar{\mathbf{z}}_k. \end{aligned} \tag{48}$$

Fortunately, the effective channel matrix $\tilde{\mathbf{H}}_k$ in (48) is full rank provided that all channel coefficients are independently drawn from a continuous distribution. As a result, it is possible to reliably decode all three data symbols in $\mathbf{s}_k$ at the k-th BS using five time slots, i.e., $d_\Sigma = \frac{3K}{5}$.

This result is a remarkable gain compared to the sum-DoF of $d_\Sigma^{\mathrm{MAC}} = \frac{K}{7}$ attained by the proposed method without considering the propagation delay (see Theorem 1). This DoF gain stems from the additional use of ICI-free received signals during the delay in ICI links; this essentially increases the rank of the effective channel matrix after the ICI cancellation.

B. Propagation Delay With $L_{D,k} \le L_{I,k}$

When the propagation delay exists, the delay spread of the ICI links may larger than that of the desired links, i.e., $L_{\mathrm{D},k} \le L_{\mathrm{I},k}$, as depicted in Fig. 4(c). In this case, Theorem 1 implies that without CSIT, the sum-DoF cannot be scaled linearly with the number of the cells, K. Nevertheless, it is still possible to apply the proposed interference management method to obtain a spectral efficiency gain instead. The basic idea is to consider a fraction of ICI signals as *effective ICI* signals, while treating the remaining ICI signals as additional noise. For example, the last $L_\mathrm{I} - L_\mathrm{D}$ CIR taps of ICI links can be treated as noise, so that the blind interference management method is applicable for the system. In what follows, we validate the effectiveness of this alternative approach by using a numerical example with simulations.

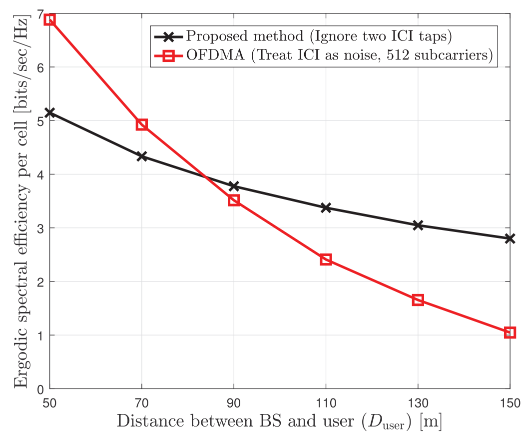

Fig. 5. Ergodic spectral efficiencies per cell of the proposed interference management method and OFDMA for different distances (D_{user}) between a BS and each user. 7-cell deployment illustrated in Fig. 6 is considered with $D_{\mathrm{site}} = 300$ m. The performance of the center cell is plotted. Total transmission power at the user and the noise power are set as -174 dBm/Hz and 23 dBm, respectively. Other parameters are specified in Example 3.

Example 3(Approximate Method for Propagation Delay With $L_{D,k} \le L_{I,k}$): We consider the same scenario with Example 2, but set the number of CIR taps for ICI links to be $L_{\mathrm{I},k} = L_\mathrm{I} = 6$, which is larger than $L_{\mathrm{D},k} = L_\mathrm{D} = 4$ for $k \in \mathcal{K}$, as depicted in Fig. V(c). We intentionally treat the last two CIR taps of ICI links as noise, then apply the same transmission/reception strategy presented in Example 2. The only change is that each user appends two zeros at the end of the subblock transmission to prevent the inter-subblock-interference caused by the ICI links. In Fig. 5, using simulation, we plot ergodic spectral efficiency per cell attained by using this alternative approach. For the performance comparison, we also plot the spectral efficiency of a conventional OFDMA strategy that treats all ICI signals as noise. We adopt a distance-based large-scale fading model in which a path loss exponent is given by $\alpha = 4$ and the reference path loss at 1 meter is set as $P_0 = -80$ dB. We also model the ℓ-th tap of the CIR between user (i,u) and the k-th BS by $h_{k,u}[\ell] = \sqrt{P_0} d_{k,k,u}^{-\frac{\alpha}{2}} \check{h}_{k,u}[\ell]$ for $i = k$ and $g^{k}_{i,u}[\ell] = \sqrt{P_0} d_{k,i,u}^{-\frac{\alpha}{2}} \check{g}^{k}_{i,u}[\ell]$ for $i \ne k$, where $d_{k,i,u}$ is the distance (in meters) between user (i,u) and the k-th BS, and both $\check{h}_{k,u}[\ell]$ and $\check{g}^{k}_{i,u}[\ell]$ are IID as $\mathcal{CN}(0, \gamma_{k,i,\ell})$. We assume that $\gamma_{k,i,\ell}$ follows the exponentially-decaying power-delay profile (PDP) with a decaying constant 0.5.

Fig. 5 shows that when ICI is dominant, the proposed interference management method outperforms OFDMA. This implies that the proposed interference management method effectively mitigates ICI even if we ignore some CIR taps of ICI links. Whereas, when the users are close to the BS, ICI is no longer a dominant factor, so the spectral efficiency of the proposed interference management method becomes lower than that of OFDMA which treats ICI as noise. From this numerical example, it is concluded that the proposed interference management strategy can still be used as an interference-mitigation method even when $L_{\text{D}} \leq L_{\text{I}}$ case. Note that its effectiveness may heavily depend on wireless environments.

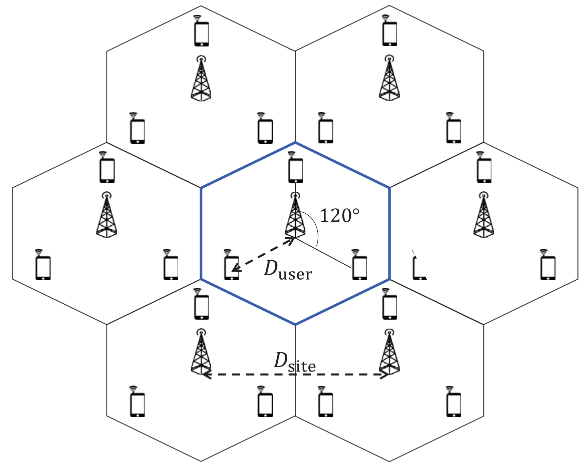

Fig. 6. Illustration of 7-cell deployment scenario with three users per cell.

VI. Extension for Heterogeneity of Channel Coherence Time

In this section, we extend the proposed interference management method to exploit the heterogeneity[1] of the channel coherence time between desired and ICI links. The proposed method has been presented under the assumption that coherence time of all links is the same. Surprisingly, when the coherence time of the desired link is shorter than that of the ICI link, the achievable sum-DoF of the proposed method can be further improved by using this new type of heterogeneity, jointly with the heterogeneity of the channel delay spreads. In the following, we demonstrate this improvement by using an illustrative example.

Example 4(Exploiting the Heterogeneity of the Channel Coherence Time): We consider a 3-cell MAC with two users per cell when $L_{\text{D},k} = 5$ and $L_{\text{I},k} = 3$ for $k \in \mathcal{K}$. We assume that each possible link between a user and a BS follows one of three different block-fading patterns that have different coherence time, as illustrated in Fig. 7. Specifically, we assume that desired links follow Type-1 fading, in which the channel coefficients are $\{h_{k,u}[n]\}$ during the first $T_1 = 5$ time slots and $\{h'_{k,u}[n]\}$ during the subsequent $T_2 = 3$ time slots. Whereas, we assume that ICI links follow Type-2 or Type-3 fading in which channel coefficients remain constant for $T_b = 8$ time slots. In this scenario,[2] we will show that each BS is able to decode four data symbols using eight time slots, i.e., $d_{\Sigma} = \frac{4}{8}K$ with $K = 3$. For this, we present a proper modification on the proposed interference management method. The major change in this modification is to use a cyclic prefix with the length of $L_{\text{I}} - 1$, instead of using the receive combining matrix such as the one in (22).

Using the transmission strategy of the proposed interference management method, user (k, u) uses the first two columns of the 6-point IDFT matrix to convey two data symbols, i.e., $\bar{\mathbf{x}}_{k,u} = \mathbf{F}_k \mathbf{s}_{k,u} \in \mathbb{C}^6$, where $\mathbf{F}_k = [\mathbf{f}_1, \mathbf{f}_2]$, $\mathbf{f}_n$ is the n-th column of the 6-point IDFT matrix, $\mathbf{s}_{k,u} = [s_{k,u,1}, s_{k,u,2}]^\top$, and $s_{k,u,m}$ is the m-th data symbol sent by user (k, u). Different from the proposed method in Section IV, the transmitted signal vector is generated by adding the cyclic prefix with the length of $L_{\text{I}} - 1 = 2$ to $\bar{\mathbf{x}}_{k,u}$. Then after removing the cyclic prefix at the receiver (i.e., removing the first two received signals), the received signal vector at the k-th BS is given as in (49) (see the bottom of the next page). It is clear that the channel matrix of the ICI link, $\bar{\mathbf{G}}^k_{i,u}$ for $i \neq k$, is circulant, while the channel matrix of the desired link, $\bar{\mathbf{H}}_{k,u}$, is noncirculant. Here, $\bar{\mathbf{H}}_{k,u}$ is decomposed as the sum of a circulant matrix and a noncirculant matrix:

$$\bar{\mathbf{H}}_{k,u} = \bar{\mathbf{H}}^{\text{C}}_{k,u} + \bar{\mathbf{H}}^{\text{NC}}_{k,u}, \tag{50}$$

where $\bar{\mathbf{H}}^{\text{C}}_{k,u} = \text{Circ}\left(\left[h_{k,u}[0], h_{k,u}[1] \cdots, h_{k,u}[4], 0\right]\right)$ and

$$\bar{\mathbf{H}}^{\text{NC}}_{k,u} = \begin{bmatrix} 0 & 0 & -h_{k,u}[4] & -h_{k,u}[3] & 0 & 0 \\ 0 & 0 & 0 & -h_{k,u}[4] & 0 & 0 \\ 0 & 0 & 0 & 0 & 0 & 0 \\ 0 & 0 & 0 & h'_{k,u}[0] & 0 & 0 \\ 0 & 0 & 0 & h'_{k,u}[1] & h'_{k,u}[0] & 0 \\ 0 & 0 & 0 & h'_{k,u}[2] & h'_{k,u}[1] & h'_{k,u}[0] \end{bmatrix}. \tag{51}$$

If a receive combining matrix defined as $\mathbf{W} = [\mathbf{f}_3, \mathbf{f}_4, \mathbf{f}_5, \mathbf{f}_6]^H$ is applied to the received signal in (49), the effective received signal at the k-th BS, namely $\tilde{\mathbf{y}}_k \in \mathbb{C}^4$, is obtained as

$$\begin{aligned} \tilde{\mathbf{y}}_k &= \mathbf{W}\bar{\mathbf{y}}_k = \sum_{u=1}^{2} \mathbf{W}\bar{\mathbf{H}}_{k,u}\mathbf{F}_k\mathbf{s}_{k,u} + \sum_{i \neq k}\sum_{u=1}^{2} \mathbf{W}\bar{\mathbf{G}}^k_{i,u}\mathbf{F}_k\mathbf{s}_{i,u} + \mathbf{W}\bar{\mathbf{z}}_k \\ &= \sum_{u=1}^{2} \mathbf{W}\bar{\mathbf{H}}^{\text{NC}}_{k,u}\mathbf{F}_k\mathbf{s}_{k,u} + \mathbf{W}\bar{\mathbf{z}}_k \\ &= \underbrace{\left[\mathbf{W}\bar{\mathbf{H}}^{\text{NC}}_{k,1}\mathbf{F}_k, \mathbf{W}\bar{\mathbf{H}}^{\text{NC}}_{k,2}\mathbf{F}_k\right]}_{\tilde{\mathbf{H}}_k} \begin{bmatrix} \mathbf{s}_{k,1} \\ \mathbf{s}_{k,2} \end{bmatrix} + \mathbf{W}\bar{\mathbf{z}}_k. \end{aligned} \tag{52}$$

[1]The heterogeneity of the channel coherence time has originally been considered in [31]–[33] and exploited for developing the blind interference alignment technique.

[2]This scenario could be impractical because in general, the coherence time of wireless channels such as T_1, T_2, and T_b is much larger than the values considered in this scenario. Nevertheless, this scenario is considered only to present a simple example for the extension of the proposed method. It should also be noticed that when the values of $L_{\text{D},k}$ and $L_{\text{I},k}$ are lower than the coherence time, we can adopt multiple subblock transmission as explained in Section IV.

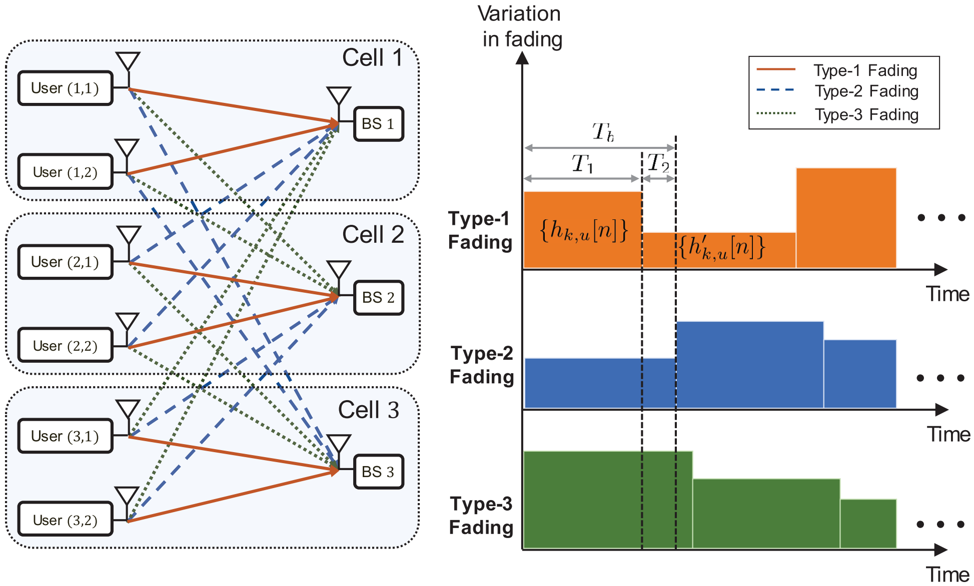

Fig. 7. Example of a 3-cell MAC with two users per cell when the heterogeneity of the channel coherence time exists.

The rank of the effective channel matrix $\tilde{\mathbf{H}}_k \in \mathbb{C}^{4\times 4}$ is four with probability one, provided that all channel coefficients are independently drawn from a continuous distribution. As a result, for every user, two data symbols are reliably decoded at the associating BS. Because eight time slots are consumed to decode two data symbols per user, the achievable sum-DoF is given by $d_\Sigma = \frac{4}{8}K = \frac{3}{2}$.

The above example clearly shows that the modified method using the cyclic prefix improves the achievable sum-DoF compared to the proposed method in Section IV which achieves the sum-DoF of $d_\Sigma^{\mathrm{MAC}} = 1$ (see Theorem 1). This DoF gain is obtained by exploiting the heterogeneity of the channel coherence time between the desired and ICI links, in addition to the heterogeneity of the channel delay spreads.

VII. Conclusion

In this work, we showed that the interference-free sum-DoF of K is asymptotically achievable in a K-cell SISO MAC with ISI, even in the absence of CSIT. This achievability was demonstrated by a blind interference management method that exploits the relativity in delay spreads between desired and interfering links. The result of this work is surprising because the existing work on multi-cell MAC has been shown to asymptotically achieve the sum-DoF of K only when global and perfect CSIT are available [15], [16]. We also observed that a significant DoF gain compared to the result in [34] is obtained when multiple users exist in a cell by improving the utilization of signal dimensions.

The proposed interference management method can be extended to characterize the achievable sum-DoF of a K-cell

$$\underbrace{\begin{bmatrix} y_k[3]\\ y_k[4]\\ y_k[5]\\ y_k[6]\\ y_k[7]\\ y_k[8]\end{bmatrix}}_{\bar{\mathbf{y}}_k} = \sum_{u=1}^{2} \underbrace{\begin{bmatrix} h_{k,u}[0] & 0 & 0 & 0 & h_{k,u}[2] & h_{k,u}[1]\\ h_{k,u}[1] & h_{k,u}[0] & 0 & 0 & h_{k,u}[3] & h_{k,u}[2]\\ h_{k,u}[2] & h_{k,u}[1] & h_{k,u}[0] & 0 & h_{k,u}[4] & h_{k,u}[3]\\ h_{k,u}[3] & h_{k,u}[2] & h_{k,u}[1] & h'_{k,u}[0] & 0 & h_{k,u}[4]\\ h_{k,u}[4] & h_{k,u}[3] & h_{k,u}[2] & h'_{k,u}[1] & h'_{k,u}[0] & 0\\ 0 & h_{k,u}[4] & h_{k,u}[3] & h'_{k,u}[2] & h'_{k,u}[1] & h'_{k,u}[0] \end{bmatrix}}_{\bar{\mathbf{H}}_{k,u}} \begin{bmatrix} x_{k,u}[1]\\ x_{k,u}[2]\\ x_{k,u}[3]\\ x_{k,u}[4]\\ x_{k,u}[5]\\ x_{k,u}[6]\end{bmatrix}$$

$$+ \sum_{i\neq k}\sum_{u=1}^{2} \underbrace{\begin{bmatrix} g_{i,u}^k[0] & 0 & 0 & 0 & 0 & g_{i,u}^k[1]\\ g_{i,u}^k[1] & g_{i,u}^k[0] & 0 & 0 & 0 & 0\\ 0 & g_{i,u}^k[1] & g_{i,u}^k[0] & 0 & 0 & 0\\ 0 & 0 & g_{i,u}^k[1] & g_{i,u}^k[0] & 0 & 0\\ 0 & 0 & 0 & g_{i,u}^k[1] & g_{i,u}^k[0] & 0\\ 0 & 0 & 0 & 0 & g_{i,u}^k[1] & g_{i,u}^k[0] \end{bmatrix}}_{\bar{\mathbf{G}}_{i,u}^k} \begin{bmatrix} x_{i,u}[1]\\ x_{i,u}[2]\\ x_{i,u}[3]\\ x_{i,u}[4]\\ x_{i,u}[5]\\ x_{i,u}[6]\end{bmatrix} + \underbrace{\begin{bmatrix} z_k[3]\\ z_k[4]\\ z_k[5]\\ z_k[6]\\ z_k[7]\\ z_k[8]\end{bmatrix}}_{\mathbf{z}_k}. \tag{49}$$

broadcast channel (or interfering broadcast channel) by using the uplink-downlink relation of the MAC and the broadcast channel. Therefore, it would be interesting to investigate the sum-DoF of the K-cell broadcast channel with ISI in the absence of CSIT as a future work. Another promising direction for future work is to extend the proposed interference management method for a multi-antenna setting, i.e., K-cell MIMO MAC with ISI. In this extension, it may be able to further improve the sum-DoF by exploiting additional signal dimensions provided by the use of multiple antennas. The proposed method can also be applied to derive a secure DoF for multi-cell MAC with ISI by extending an approach developed in [36].

Appendix
Proof of Lemma 2

In this proof, we show that the rank of the effective channel matrix $\tilde{\mathbf{H}}_k \in \mathbb{C}^{(N-M_{\rm D})\times U_k' M_k}$ defined in (32) is $U_k' M_k$. Because $U_k' M_k \le \Delta_k \le N - M_{\rm D}$ by the definitions, we can equivalently show that $\tilde{\mathbf{H}}_k$ is a full column rank matrix. For this, we first introduce the *rank-equivalent* representation of $\tilde{\mathbf{H}}_k$ and then use this representation to determine the rank of $\tilde{\mathbf{H}}_k$.

The rank-equivalent representation of $\tilde{\mathbf{H}}_k$ is obtained as follows. Let $\mathbf{h}_{k,u}^{\rm eff} \in \mathbb{C}^{\Delta_k}$ be an effective channel-coefficient vector of user (k,u), defined as $\mathbf{h}_{k,u}^{\rm eff} = \Big[h_{k,u}[L_{{\rm I},k}], \cdots, h_{k,u}[L_{{\rm D},k} - 1]\Big]^\top$. Using this vector, $\mathbf{W}\bar{\mathbf{H}}_{k,u}^{\rm NC}\mathbf{f}_m$ can be decomposed as

$$\mathbf{W}\bar{\mathbf{H}}_{k,u}^{\rm NC}\mathbf{f}_m = \mathbf{W}\mathbf{E}_{m,k}\mathbf{h}_{k,u}^{\rm eff}. \tag{53}$$

In the above decomposition, $\mathbf{E}_{m,k} \in \mathbb{C}^{N\times\Delta_k}$ is a matrix with the special form:

$$\mathbf{E}_{m,k} = \begin{bmatrix} \mathbf{0}_{(L_{{\rm D},k}-N_k')\times(N_k'-L_{{\rm I},k})} & \mathbf{E}_{m,k}^{\rm low} \\ \mathbf{0}_{(N_k'-\Delta_k-1)\times(N_k'-L_{{\rm I},k})} & \mathbf{E}_{m,k}^{\rm rect} \\ \mathbf{E}_{m,k}^{\rm upp} & \mathbf{0}_{(N_k'-L_{{\rm I},k})\times(L_{{\rm D},k}-N_k')} \\ \mathbf{0}_{(N-N_k'+1)\times(N_k'-L_{{\rm I},k})} & \mathbf{0}_{(N-N_k'+1)\times(L_{{\rm D},k}-N_k')} \end{bmatrix}, \tag{54}$$

where $\mathbf{E}_{m,k}^{\rm low} \in \mathbb{C}^{(L_{{\rm D},k}-N_k')\times(L_{{\rm D},k}-N_k')}$ is a lower triangular matrix given by

$$\mathbf{E}_{m,k}^{\rm low} = \begin{bmatrix} 1 & & & \\ w_m & \ddots & & \\ \vdots & \ddots & \ddots & \\ w_m^{L_{{\rm D},k}-N_k'-1} & \cdots & w_m & 1 \end{bmatrix}, \tag{55}$$

$\mathbf{E}_{m,k}^{\rm upp} \in \mathbb{C}^{(N_k'-L_{{\rm I},k})\times(N_k'-L_{{\rm I},k})}$ is an upper triangular matrix given by

$$\mathbf{E}_{m,k}^{\rm upp} = \begin{bmatrix} -w_m^N & -w_m^{N-1} & \cdots & -w_m^{L_{{\rm I},k}+1} \\ & \ddots & \ddots & \vdots \\ & & \ddots & -w_m^{N-1} \\ & & & -w_m^N \end{bmatrix}, \tag{56}$$

$\mathbf{E}_{m,k}^{\rm rect} \in \mathbb{C}^{(N_k'-\Delta_k-1)\times(L_{{\rm D},k}-N_k')}$ is a rectangular matrix given by

$$\mathbf{E}_{m,k}^{\rm rect} = \begin{bmatrix} w_m^{L_{{\rm D},k}-N_k'} & w_m^{L_{{\rm D},k}-N_k'-1} & \cdots & w_m \\ w_m^{L_{{\rm D},k}-N_k'+1} & w_m^{L_{{\rm D},k}-N_k'} & \cdots & w_m^2 \\ \vdots & \vdots & & \vdots \\ w_m^{L_{{\rm I},k}-2} & w_m^{L_{{\rm I},k}-3} & \cdots & w_m^{N_k'-\Delta_k-1} \end{bmatrix}, \tag{57}$$

and $w_m = e^{j\frac{2\pi}{N}(m-1)}$. From (53), the rank of $\tilde{\mathbf{H}}_k$ is represented as

$$\begin{aligned} &{\rm rank}(\tilde{\mathbf{H}}_k) \\ &= {\rm rank}\Big(\Big[\mathbf{W}\bar{\mathbf{H}}_{k,1}^{\rm NC}\mathbf{F}_k, \mathbf{W}\bar{\mathbf{H}}_{k,2}^{\rm NC}\mathbf{F}_k, \cdots, \mathbf{W}\bar{\mathbf{H}}_{k,U_k'}^{\rm NC}\mathbf{F}_k\Big]\Big) \\ &= {\rm rank}\Big(\Big[\mathbf{W}\mathbf{E}_{1,k}\mathbf{h}_{k,1}^{\rm eff}, \cdots, \mathbf{W}\mathbf{E}_{M_k,k}\mathbf{h}_{k,1}^{\rm eff}, \\ &\qquad \cdots, \mathbf{W}\mathbf{E}_{1,k}\mathbf{h}_{k,U_k'}^{\rm eff}, \cdots, \mathbf{W}\mathbf{E}_{M_k,k}\mathbf{h}_{k,U_k'}^{\rm eff}\Big]\Big). \end{aligned} \tag{58}$$

The above representation implies that $\tilde{\mathbf{H}}_k$ is a full column rank matrix if all vectors in the right-hand-side of the last equality in (58) are linearly independent. Since the elements of $\mathbf{h}_{k,u}^{\rm eff}$ are independently drawn from a continuous distribution, these vectors are linearly independent with probability one, if 1) the vectors in $\Big\{\mathbf{W}\mathbf{E}_{m,k}\mathbf{h}_{k,u}^{\rm eff}\Big\}_{m=1}^{M_k}$ are linearly independent for each $u \in \mathcal{U}_k'$, and also if 2) $\mathbf{W}\mathbf{E}_{m,k}$ is a full column rank matrix for $m \in \{1,2,\ldots,M_k\}$. In what follows, we will show that these two conditions hold, by utilizing the property of the DFT matrix and a well-known rank inequality.

First, we show that $\Big\{\mathbf{W}\mathbf{E}_{m,k}\mathbf{h}_{k,u}^{\rm eff}\Big\}_{m=1}^{M_k}$ are linearly independent, i.e.,

$${\rm rank}\Big(\Big[\mathbf{W}\mathbf{E}_{1,k}\mathbf{h}_{k,u}^{\rm eff}, \mathbf{W}\mathbf{E}_{2,k}\mathbf{h}_{k,u}^{\rm eff}, \cdots, \mathbf{W}\mathbf{E}_{M_k,k}\mathbf{h}_{k,u}^{\rm eff}\Big]\Big) = M_k, \tag{59}$$

for each $u \in \mathcal{U}_k'$. Note that from (53), we have $\mathbf{W}\bar{\mathbf{H}}_{k,u}^{\rm NC}\mathbf{F}_k = \Big[\mathbf{W}\mathbf{E}_{1,k}\mathbf{h}_{k,u}^{\rm eff}, \cdots, \mathbf{W}\mathbf{E}_{M_k,k}\mathbf{h}_{k,u}^{\rm eff}\Big]$. Therefore, for the proof of (59), we instead show that the rank of $\mathbf{W}\bar{\mathbf{H}}_{k,1}^{\rm NC}\mathbf{F}_k$ is M_k by using the following lemma:

Lemma 3: For a matrix $\mathbf{ABC}$ defined by the product of three matrices $\mathbf{A}$, $\mathbf{B}$, and $\mathbf{C}$, the following inequality holds:

$${\rm rank}(\mathbf{AB}) + {\rm rank}(\mathbf{BC}) \le {\rm rank}(\mathbf{B}) + {\rm rank}(\mathbf{ABC}). \tag{60}$$

Proof: See [37]. ■

Lemma 3 implies that if we determine the ranks of three matrices $\mathbf{W}\bar{\mathbf{H}}_{k,u}^{\rm NC}$, $\bar{\mathbf{H}}_{k,u}^{\rm NC}\mathbf{F}_k$, and $\bar{\mathbf{H}}_{k,u}^{\rm NC}$, we can directly obtain an inequality condition for the rank of $\mathbf{W}\bar{\mathbf{H}}_{k,u}^{\rm NC}\mathbf{F}_k$ from (60). Fortunately, by the definition of $\bar{\mathbf{H}}_{k,u}^{\rm NC}$ given in (27), the rank of $\bar{\mathbf{H}}_{k,u}^{\rm NC}$ is Δ_k. Furthermore, the ranks of $\mathbf{W}\bar{\mathbf{H}}_{k,u}^{\rm NC}$ and $\bar{\mathbf{H}}_{k,u}^{\rm NC}\mathbf{F}_k$ can be determined by using the property of the submatrix of the DFT matrix: Any N_2 columns of an N_1 by N submatrix of the N-point DFT matrix, constructed by removing $N - N_1$ consecutive rows from the original DFT matrix, are linearly independent when $N - N_1 \ge N_2$; this property can easily be shown by extending the result in [38] (see Appendix C in [38]). Because $\mathbf{W} = \left[\mathbf{f}_{M_{\mathrm{D}}+1}, \cdots, \mathbf{f}_N\right]^H$ and $\mathbf{F}_k^H = \left[\mathbf{f}_1, \mathbf{f}_2, \cdots, \mathbf{f}_{M_k}\right]^H$ are the submatrices of the N-point DFT matrix, the above property implies that any $L_{\mathrm{D},k} - L_{\mathrm{I}}$ columns of $\mathbf{W}$ are linearly independent, and also that any M_k columns of $\mathbf{F}_k^H$ are linearly independent. Using these facts along with the definition of $\bar{\mathbf{H}}_{k,u}^{\mathrm{NC}}$, we have

$$\mathrm{rank}(\mathbf{W}\bar{\mathbf{H}}_{k,u}^{\mathrm{NC}}) = \Delta_k, \tag{61}$$

$$\mathrm{rank}(\bar{\mathbf{H}}_{k,u}^{\mathrm{NC}}\mathbf{F}_k) = \mathrm{rank}(\mathbf{F}_k^H(\bar{\mathbf{H}}_{k,u}^{\mathrm{NC}})^H) = M_k. \tag{62}$$

Plugging the above results to (60) yields $M_k \leq \mathrm{rank}(\mathbf{W}\bar{\mathbf{H}}_{k,u}^{\mathrm{NC}}\mathbf{F}_k)$. Because $\mathbf{W}\bar{\mathbf{H}}_{k,u}^{\mathrm{NC}}\mathbf{F}_k$ is a tall matrix with M_k columns, the rank of $\mathbf{W}\bar{\mathbf{H}}_{k,u}^{\mathrm{NC}}\mathbf{F}_k$ is given by M_k, which is our desired result.

Now, we show that $\mathbf{W}\mathbf{E}_{m,k}$ is a full column rank matrix, i.e., $\mathrm{rank}\left(\mathbf{W}\mathbf{E}_{m,k}\right) = \Delta_k$, for $m \in \{1, \ldots, M_k\}$. By the structure of $\mathbf{E}_{m,k}$ in (54), every column of $\mathbf{W}\mathbf{E}_{m,k}$ contains one distinct column of $\mathbf{W}$ that is not contained in the remaining columns of $\mathbf{W}\mathbf{E}_{m,k}$. This implies that the column space of $\mathbf{W}\mathbf{E}_{m,k}$ contains a space spanned by Δ_k different columns of $\mathbf{W}$. In the previous discussion, we have already shown that any Δ_k columns of $\mathbf{W}$ are linearly independent. Therefore, the dimension of the column space of $\mathbf{W}\mathbf{E}_{m,k}$ is Δ_k, and consequently, $\mathbf{W}\mathbf{E}_{m,k}$ is a full column rank matrix, which is our desired result.

References

[1] Y.-S. Jeon, N. Lee, and R. Tandon, "On the degrees of freedom of wideband multi-cell multiple access channels with no CSIT," in *Proc. IEEE Int. Symp. Inf. Theory (ISIT)*, Jun. 2017, pp. 2623–2627.

[2] R. W. Chang, "Synthesis of band-limited orthogonal signals for multichannel data transmission," *Bell Syst. Tech. J.*, vol. 45, no. 10, pp. 1775–1796, Dec. 1966.

[3] S. Weinstein and P. Ebert, "Data transmission by frequency-division multiplexing using the discrete Fourier transform," *IEEE Trans. Commun. Technol.*, vol. COM-19, no. 5, pp. 628–634, Oct. 1971.

[4] J. A. C. Bingham, "Multicarrier modulation for data transmission: An idea whose time has come," *IEEE Commun. Mag.*, vol. 28, no. 5, pp. 5–14, Mar. 1990.

[5] R. S. Cheng and S. Verdú, "Gaussian multiaccess channels with ISI: Capacity region and multiuser water-filling," *IEEE Trans. Inf. Theory*, vol. 39, no. 3, pp. 773–786, May 1993.

[6] C. Y. Wong, R. S. Cheng, K. B. Letaief, and R. D. Murch, "Multiuser OFDM with adaptive subcarrier, bit, and power allocation," *IEEE J. Sel. Areas Commun.*, vol. 17, no. 10, pp. 1747–1758, Oct. 1999.

[7] W. Rhee and J. M. Cioffi, "Increase in capacity of multiuser OFDM system using dynamic subchannel allocation," in *Proc. IEEE Int. Veh. Technol. Conf. (VTC)*, vol. 2. May 2000, pp. 1085–1089.

[8] D. Gesbert, S. Hanly, H. Huang, S. S. Shitz, O. Simeone, and W. Yu, "Multi-cell MIMO cooperative networks: A new look at interference," *IEEE J. Sel. Areas Commun.*, vol. 28, no. 9, pp. 1380–1408, Dec. 2010.

[9] D. Lee *et al.*, "Coordinated multipoint transmission and reception in LTE-advanced: Deployment scenarios and operational challenges," *IEEE Commun. Mag.*, vol. 50, no. 2, pp. 148–155, Feb. 2011.

[10] B. Clerckx, H. Lee, Y.-J. Hong, and G. Kim, "A practical cooperative multicell MIMO-OFDMA network based on rank coordination," *IEEE Trans. Wireless Commun.*, vol. 12, no. 4, pp. 1481–1491, Apr. 2013.

[11] H. Dahrouj and W. Yu, "Coordinated beamforming for the multicell multi-antenna wireless system," *IEEE Trans. Wireless Commun.*, vol. 9, no. 5, pp. 1748–1759, May 2011.

[12] N. Lee, D. Morales-Jimenez, A. Lozano, and R. W. Heath, "Spectral efficiency of dynamic coordinated beamforming: A stochastic geometry approach," *IEEE Trans. Wireless Commun.*, vol. 14, no. 1, pp. 230–241, Jan. 2015.

[13] S. A. Jafar and S. Shamai (Shitz), "Degrees of freedom region of the MIMO X channel," *IEEE Trans. Inf. Theory*, vol. 54, no. 1, pp. 151–170, Jan. 2008.

[14] V. R. Cadambe and S. A. Jafar, "Interference alignment and degrees of freedom of the K-user interference channel," *IEEE Trans. Inf. Theory*, vol. 54, no. 8, pp. 3425–3441, Aug. 2008.

[15] V. R. Cadambe and S. A. Jafar, "Interference alignment and the degrees of freedom of wireless X networks," *IEEE Trans. Inf. Theory*, vol. 55, no. 9, pp. 3893–3908, Sep. 2009.

[16] C. Suh and D. Tse, "Interference alignment for cellular networks," in *Proc. 46th Annu. Allerton Conf. Commun. Control Comput. (Allerton)*, Sep. 2008, pp. 1037–1044.

[17] A. Chaaban, A. Sezgin, B. Bandemer, and A. Paulraj, "On Gaussian multiple access channels with interference: Achievable rates and upper bounds," in *Proc. 4th Int. Workshop Multiple Access Commun. (MACOM)*, Sep. 2011, pp. 87–96.

[18] T. Kim, D. J. Love, B. Clerckx, and D. Hwang, "Spatial degrees of freedom of the multicell MIMO multiple access channel," in *Proc. IEEE Global Commun. Conf. (GLOBECOM)*, Dec. 2011, pp. 1–5.

[19] N. Lee, W. Shin, R. W. Heath, Jr., and B. Clerckx, "Interference alignment with limited feedback for two-cell interfering MIMO-MAC," in *Proc. IEEE Int. Symp. Wireless Commun. Syst. (ISWCS)*, Aug. 2012, pp. 566–570.

[20] H. J. Yang, W. Shin, B. C. Jung, and A. Paulraj, "Opportunistic interference alignment for MIMO interfering multiple-access channels," *IEEE Trans. Wireless Commun.*, vol. 12, no. 5, pp. 2180–2192, May 2013.

[21] Y. Zhu and D. Guo, "The degrees of freedom of isotropic MIMO interference channels without state information at the transmitters," *IEEE Trans. Inf. Theory*, vol. 58, no. 1, pp. 341–352, Jan. 2012.

[22] M. A. Maddah-Ali and D. Tse, "Completely stale transmitter channel state information is still very useful," *IEEE Trans. Inf. Theory*, vol. 58, no. 7, pp. 4418–4431, Jul. 2012.

[23] T. Gou and S. A. Jafar, "Optimal use of current and outdated channel state information: Degrees of freedom of the MISO BC with mixed CSIT," *IEEE Commun. Lett.*, vol. 16, no. 7, pp. 1084–1087, Jul. 2012.

[24] N. Lee and R. W. Heath, Jr., "Not too delayed CSIT achieves the optimal degrees of freedom," in *Proc. 50th Annu. Allerton Conf. Commun. Control Comput. (Allerton)*, Oct. 2012, pp. 1262–1269.

[25] N. Lee and R. W. Heath, Jr., "Space-time interference alignment and degree-of-freedom regions for the MISO broadcast channel with periodic CSI feedback," *IEEE Trans. Inf. Theory*, vol. 60, no. 1, pp. 515–528, Jan. 2014.

[26] R. Tandon, S. A. Jafar, S. Shamai (Shitz), and H. V. Poor, "On the synergistic benefits of alternating CSIT for the MISO broadcast channel," *IEEE Trans. Inf. Theory*, vol. 59, no. 7, pp. 4106–4128, Jul. 2013.

[27] S. A. Jafar, "Topological interference management through index coding," *IEEE Trans. Inf. Theory*, vol. 60, no. 1, pp. 529–568, Jan. 2014.

[28] C. S. Vaze and M. K. Varanasi, "The degree-of-freedom regions of MIMO broadcast, interference, and cognitive radio channels with no CSIT," *IEEE Trans. Inf. Theory*, vol. 58, no. 8, pp. 5354–5374, Aug. 2012.

[29] C. S. Vaze and M. K. Varanasi, "A new outer bound via interference localization and the degrees of freedom regions of MIMO interference networks with no CSIT," *IEEE Trans. Inf. Theory*, vol. 58, no. 11, pp. 6853–6869, Nov. 2012.

[30] S. A. Jafar, "Interference alignment—A new look at signal dimensions in a communication network," *Found. Trends Commun. Inf. Theory*, vol. 7, no. 1, pp. 1–134, 2011.

[31] C. Wang, T. Gou, and S. A. Jafar, "Aiming perfectly in the dark-blind interference alignment through staggered antenna switching," *IEEE Trans. Signal Process.*, vol. 59, no. 6, pp. 2734–2744, Jun. 2011.

[32] S. A. Jafar, "Blind interference alignment," *IEEE J. Sel. Topics Signal Process.*, vol. 6, no. 3, pp. 216–227, Jun. 2012.

[33] M. Morales-Céspedes, J. Plata-Chaves, D. Toumpakaris, S. A. Jafar, and A. G. Armada, "Blind interference alignment for cellular networks," *IEEE Trans. Signal Process.*, vol. 63, no. 1, pp. 41–56, Jan. 2015.

[34] N. Lee. (Sep. 2016). "Interference-free OFDM: Rethinking OFDM for interference networks with inter-symbol interference." [Online]. Available: http://arxiv.org/abs/1609.02517

[35] G. H. Golub and C. F. Van Loan, *Matrix Computations*, 3rd ed. Baltimore, MD, USA: The Johns Hopkins Univ. Press, 1996.

[36] J. D. Mutangana, R. Tandon, and N. Lee, "Blind cooperative jamming: Exploiting ISI heterogeneity to achieve positive secure DoF," in *Proc. IEEE Global Commun. Conf. (GLOBECOM)*, Dec. 2017, pp. 1–6.

[37] R. A. Horn and C. R. Johnson, *Matrix Analysis*, 2nd ed. Cambridge, U.K.: Cambridge Univ. Press, 2013.

[38] G. Rath and C. Guillemot, "Frame-theoretic analysis of DFT codes with erasures," *IEEE Trans. Signal Process.*, vol. 52, no. 2, pp. 447–460, Feb. 2004.

Yo-Seb Jeon received the B.S. (Hons.) and Ph.D. degrees in electronic and electrical engineering from the Pohang University of Science and Technology (POSTECH), Pohang, South Korea, in 2012 and 2016, respectively. He is currently a Post-Doctoral Researcher at POSTECH. His research interests include signal processing, machine learning algorithms, and information theory for wireless communication systems. He was a recipient of the TJ PARK Graduate Fellowship from POSTECH from 2012 to 2014.

Namyoon Lee (S'11–M'14) received the B.E. degree from Korea University, Seoul, South Korea, in 2006, the M.S. degree in electrical engineering from the Korea Advanced Institute of Science and Technology, Daejeon, in 2008, and the Ph.D. degree from the Department of Electrical and Computer Engineering, The University of Texas at Austin, in 2014. From 2008 to 2011, he was with the Samsung Advanced Institute of Technology, South Korea, where he designed next generation wireless communication systems and involved standardization activities of the 3GPP LTE-A. He was also with the Nokia Research Center at Berkeley as a Senior Researcher, where he participated in the design of future WLAN systems (e.g., IEEE 802.11ax and 802.11ay) from 2014 to 2015. He was with Wireless Communications Research at Intel Laboratories, Santa Clara, CA, USA, as a Research Scientist from 2015 to 2016. He is currently an Assistant Professor with the Department of Electrical Engineering, POSTECH. His current research interest is to develop and analyze future wireless communication systems using tools, including multi-antenna network information theory, stochastic geometry, and machine learning algorithms.

Mr. Lee was a recipient of the 2016 IEEE ComSoc Asia-Pacific Outstanding Young Researcher Award, the 2009 Samsung Best Paper Award, the 2014 Student Best Paper Award (IEEE Seoul Section), and the Recognition Award from Intel Labs 2015. He was also an Exemplary Reviewer of the IEEE WIRELESS COMMUNICATIONS LETTERS in 2013 and 2015.

Ravi Tandon (SM'17) received the B.Tech. degree in electrical engineering from IIT Kanpur in 2004, and the Ph.D. degree in electrical and computer engineering from the University of Maryland, College Park (UMCP), in 2010. From 2010 to 2012, he was a Post-Doctoral Research Associate with the Department of Electrical Engineering, Princeton University. He is currently an Assistant Professor with the Department of Electrical and Computer Engineering, University of Arizona. Prior to joining the University of Arizona in fall 2015, he was a Research Assistant Professor at Virginia Tech with positions in the Bradley Department of ECE, the Hume Center for National Security and Technology, and the Discovery Analytics Center in the Department of Computer Science. His current research interests include information theory and its applications to wireless networks, communications, security and privacy, distributed storage, machine learning, and data mining. He was a co-recipient of the Best Paper Award at the IEEE GLOBECOM 2011. He was nominated for the Graduate School Best Dissertation Award, and also for the ECE Distinguished Dissertation Fellowship Award at UMCP. He received the NSF CAREER Award in 2017.